

5086

ANNUAL REPORT

Contract Number: 03-5-022-55
Research Unit Numbers: 253, 244, 256
OCSEAP Task Numbers: D8 and D9
Reporting Period: April 1, 1981 to
March 31, 1982

2313
3964

SUBSEA PERMAFROST:
PROBING, THERMAL REGIME AND DATA ANALYSIS

T. E. Osterkamp
W. D. Harrison

Geophysical Institute
University of Alaska
Fairbanks, Alaska 99701

JIM LANE

TABLE OF CONTENTS

		Page
I.	SUMMARY OF OBJECTIVES, CONCLUSIONS AND IMPLICATIONS	1
II.	INTRODUCTION	1
III.	CURRENT STATE OF KNOWLEDGE	2
IV*	S T U D Y A R E A	2
V.	METHODS AND RATIONALE OF DATA COLLECTION	2
VI.& VII.	RESULTS AND DISCUSSION	3
	A. Chukchi Sea	
	B. Beaufort Sea	
	C. Barrier Islands	
VIII.	SUMMARY AND CONCLUSIONS	24
IX.	ACKNOWLEDGEMENTS	
X.	REFERENCES; FIGURES AND TABLES	
XI.	APPENDICES	
	Appendix A: Temperature Data	
	Appendix B: Sediment in Sea Ice Studies	
	Appendix C: Publications	

I. SUMMARY OF OBJECTIVES, CONCLUSIONS AND IMPLICATIONS WITH RESPECT TO OCS DEVELOPMENT

The objectives of this study are to determine the occurrence, distribution and properties of subsea permafrost in Alaskan waters in cooperation with other OCSEAP investigators. Besides direct measurements, our program includes an effort to understand the basic physical processes responsible for the subsea permafrost regime, as a basis for predictive models.

The detailed conclusions of our 1981 field work are in Section VIII. Our data in the Chukchi Sea are insufficient to allow us to assess the occurrence, distribution and characteristics of subsea permafrost as a hazard to OCS development. Additional research is required to determine the presence of rock near the sea bed and to determine whether or not the rock contains segregated ice. Shallow ice-bearing permafrost in the Beaufort Sea (Harrison Bay and westward) will create severe problems for bottom-founded structures and pipelines.

It is likely that problems posed by subsea permafrost for offshore hot oil production will be greater than for permafrost problems onshore at Prudhoe Bay, because subsea permafrost is warmer, saltier and more easily disturbed, and because it is often associated with fine-grained soils.

II. INTRODUCTION

This work is part of the OCSEAP study of the distribution and properties of permafrost beneath the seas adjacent to Alaska and of processes that control the evolution of the subsea permafrost. The study involves coordination of the efforts of a number of investigators (RU 204, 271, 253, 255, 256, 473, 103, 407) and synthesis of the results of both field and laboratory work. Related

work that is more focused on the scientific problems of heat and mass transfer in subsea permafrost is primarily funded by the National Science Foundation and supported by OCSEAP Logistics.

More information on specific objectives, and relevance to problems of petroleum development, are given in our previous annual reports.

111. CURRENT STATE OF KNOWLEDGE

A summary of the current state of knowledge was given in Section III and Appendix B of a previous report (Osterkamp and Harrison, 1980), and by the other OCSEAP investigators in their reports. A detailed summary will also be prepared this year as part of our final report.

IV. STUDY AREA

Field investigations were carried out in the following areas in 1981: Chukchi Sea between Wainwright and Kotzebue, Beaufort Sea west of Cape Halkett, Atigaru Point, Harrison Bay and Prudhoe Bay and on Thetis, Reindeer, Cross and Flaxman Islands.

v. METHODS AND RATIONALE OF DATA COLLECTION

Although there have been some refinements, our methods have not changed greatly from those described in our report (Osterkamp and Harrison, 1980). We have recently published two papers (Harrison and Osterkamp, 1981; Osterkamp and Harrison, 1981) that give a fairly complete description of most of the methods. Successful measurements of the pressure profile in the sediments were conducted this year at Prudhoe Bay for the first time. The method is discussed further in sections VI and VII.

VI. & VII. RESULTS AND DISCUSSION

A. Chukchi Sea

Drilling and probing data in the Chukchi Sea are very sparse. We have drilled a few holes in the northern Chukchi Sea, near the Naval Arctic Research Laboratory (NARL), two holes north of Wainwright, one hole at Rabbit Creek and two holes near Kotzebue. These holes are not sufficient to develop an understanding of the presence and distribution of subsea permafrost in the Chukchi Sea lease sale areas.

1. Cape Lisbourne

During our Spring, 1981 field season we attempted to drill six holes in the general area between Cape Lisbourne and Point Lay. Figure 1 shows the location of these holes and Table 1 contains additional information about them. In all six holes, we encountered what appeared to be bedrock within 1/2 m of the sea bed which was overlain by a thin layer of fine-grained sediment. This rock could not be penetrated with the equipment at hand, although a small modification of our present equipment would allow us to make boreholes in rock.

2. Ogotoruk Creek

We attempted to drill one hole at a site ≈ 75 m offshore in 6.40 m of water. Figure 2 shows the location and additional information is given in Table 1. The sea bed at this site was hard, apparently rock, but was not covered by sediment.

The above data and our previous field data, while very sparse, suggest that there is rock at or near the sea bed in the area along

the **Chukchi** Sea coast between Peard Bay and **Ogotoruk** Creek. Rock was not **found** at NARL (NE of Peard Bay) nor at Rabbit Creek, SE of **Ogotoruk** Creek.

The presence of rock at **or** near the sea bed poses several problems for **OCS development**. First, it cannot be assumed that the rock does not contain segregated **ice**. Both temperature profiles or borehole heating data **will** be required to determine the presence or absence of ice **in** the rock. Second, the rock cannot **be** assumed to be a good foundation material for structures unless **it** can be shown that it **does** not contain segregated ice. Third, laying pipelines in this rock could be extremely difficult. Fourth, if the rock is as widespread as our sparse data suggests then it may be very difficult to obtain gravel for construction of docks, causeways, artificial islands, etc.

In summary, our present data base in the **Chukchi** Sea is insufficient to allow us to assess the occurrence, distribution and characteristics of subsea permafrost as a hazard to **OCS** development. Additional research is required to determine the occurrence and distribution of rock permafrost at or near the sea bed and to determine whether or not the rock permafrost contains segregated ice.

B. Beaufort Sea

1. **Esook** Holes (A, **B**, **C**)

Three holes were drilled to the **NW** of Cape Halkett and east of *the* abandoned Esook Trading Post as shown in Fig. 3. Additional data are **given** in Table 1.

Hole A was drilled in 2.72 m of water on May 1, 1981. The measured sea bed temperatures suggest nearly normal sea water salinities under the ice at this time. Sea bed sediments were fine-grained. The temperature profile shown in Fig. 4 was obtained on May 29 and is probably within a few hundredths degree of equilibrium. There is a distinct change in slope of the temperature profile at the 15 m depth. Drilling was noted to be harder below this depth. A similar change in slope was noted in hole B at the 13 m depth which suggests that there may be a common change of lithology at these depths. In hole A, there is also an apparent break in the temperature profile at the 9 m depth, however, this could also be interpreted as a continuing curvature of the profile above and below this depth due to variable ice content in the sediments. A borehole heating experiment suggests that the sediments are ice-bearing, and probably ice-bonded, below ≈ 4 m where the temperature was -1.9°C .

Hole B was drilled in 5.45 m of water on May 7, 1981. Sea bed temperatures suggest that the salinity under the ice was slightly less than normal. The sediments were fine-grained. Figure 5 is a temperature profile measured on May 29th. There is a distinct break in the temperature gradient at ≈ 13 m which may represent a change in lithology as noted in Hole A. A borehole heating experiment suggests that the sediments were ice-bearing below ≈ 5 m and probably ice-bonded below ≈ 7 m. At the 5 m depth, the temperature was $\approx -1.75^{\circ}\text{C}$.

Hole C was drilled in 10.50 m of water on May 7, 1981. It was the deepest hole drilled to date (42.77 m). The sediments were **fine-grained**. Unfortunately the pipe was broken before the hole could be logged. Judging from the drilling information the **sediments** were ice-bonded relatively close to the sea bed.

The presence of ice-bearing or ice-bonded permafrost in these holes, near the sea bed, would make it difficult to lay pipelines in the sea bed and would probably require expensive construction technology that does not yet exist.

2. Atigaru Point Hole

The hole at **Atigaru Point** was drilled on May 1, 1982. It is located ≈ 10 km NE of **Atigaru Point** in 6.8 m of water. Additional data can be found in Table 1. **Fine-grained** sediments with some sand were encountered during drilling. The measured sea bed temperatures suggest slightly less than normal sea water salinities during May, 1982. Problems with the temperature data made it difficult to obtain an equilibrium temperature profile. The temperature profile shown in Fig. 6 was obtained on May 21st and is probably within a few hundredths degree of equilibrium. The mean annual sea bed temperature (MASBT) was $\approx -1.2^{\circ}\text{C}$. A borehole heating experiment, Fig. 7, suggests that the sediments are **ice-bearing** below 12 m. This is in reasonable agreement with the drilling information. The temperature at the top of the ice-bearing permafrost (12 m) was -1.36°C , which is extremely warm.

The presence of ice-bearing sediments so close to the sea bed suggests that there will be severe problems for petroleum development in the area as noted earlier.

3. Thetis Island Holes (A, B)

Two holes were drilled north of Thetis Island at positions shown in Fig. 3. Additional data are given in Table 1. Results from a hole drilled on Thetis Island are described in a later section.

Hole A was drilled in 25.92 m of water on April 30, 1981. The sea bed was thought to be soft but the drilling was slow. A total depth of \approx 5 m was reached, however the hole was lost during the casing process so that no logs were obtained.

Hole B was drilled in 14.78 m of water on April 30, 1981. The sea bed was thought to be soft and drilling was fast for the first few meters but then became slower. Sea bed temperature was \approx -1.75°C suggesting slightly less than normal sea water salinities at this site. Figure 8 is the only measured temperature profile and was obtained on May 29th. It is somewhat surprising that this profile is not "smoother". The MASBT is roughly -1.4°C. There is a change in the thermal gradient at \approx 12 m suggesting the possible presence of ice in the sediments below this depth. The hole was not deep enough to confirm this idea, however the driller noted that the hole bottom was hard and possibly frozen.

4. Prudhoe Bay - West Dock Holes

Additional experiments were performed during the 1981 field season in an effort to develop a more detailed understanding of the

heat and salt transport processes in **subsea** permafrost. **These** experiments were conducted along the line extending from the North **Prudhoe** Bay State #1 well toward Reindeer Island that was established in our 1975 season. The measurements included temperature, pore water concentration, pressure and depth to the ice-bonded permafrost boundary. **The** measurements were made in **holes** between 398 m and 448 m offshore. Hole designations are the distances offshore. They can be compared to previous measurements along this line by taking the shoreline movement into account. The hole locations are shown in Fig. 9 and additional data given in **Table 1**.

4a. Temperature Data

Holes 398, 418, 433, 439, and 448 were driven to detect the position of the ice-bonded permafrost **table** and to determine its temperature. In hole 398, for an unknown reason, the cable did not reach the bottom of the hole. The temperature in the ice 0.16 m above the sea bed at this site warmed from **-2.27°C** on June 1st to **-1.53°C** on June 2nd. It is conceivable that this warming was associated with an overflow of the **Sagavanirktok** River which had approached to **≈ 1 km** of our study site a few days earlier or it may be an error in the reading.

Figure 10 shows the temperature profile in Hole **418** measured on June 2nd. The equilibrium temperature profile is probably colder by a few **hundredths** degree. This profile is nearly linear below 3 m suggesting that the temperature at the sea bed must have remained constant at about **-1.8°C** from the **time** of freeze-up until a few

weeks **prior** to the time of this logging. **MASBT** is $\approx -1.8^{\circ}\text{C}$ although there **is** considerable uncertainty in this **value** with **such** a shallow hole.

Figure **11** shows the measured temperature profile in hole 433 on June 2nd. The equilibrium temperature profile is probably colder by a few **hundreths degree**. At 4.53 m, the temperature is about **0.07°C warmer** than a point that would **fall** on a smooth curve through the rest of the data points. **It** was also warmer on a previous logging suggesting that the temperature is anomalously warmer at this depth for some unknown reason. There is **also** what appears to be a break or a slight curvature **in** this profile between 6 and 11 m suggesting a downward flux of warmer pore water with a velocity of a few tenths meters per year, colder than normal sea bed temperatures or a change **in lithology**.

Hole 439 was driven in a hole that had been previously used for sampling sediment pore water. Figure 12 is the temperature profile measured *on* June 2nd. The equilibrium temperature profile is probably colder by a a few hundredths of a degree. **It** suggests a **MASBT** of $\approx -1.4^{\circ}\text{C}$. There is a **distinct** curvature or change in gradient between 7-14 m which could be interpreted as resulting from a downward flux of warmer water, colder than normal sea bed temperatures or a change in **lithology**. Temperature profiles obtained during the 1980 field season showed an upward curvature in contrast to the downward curvature found in 1981. These curved temperature profiles could be a result of convection **cells** in the thawed **subsea** permafrost,

"which seems likely, or they could be produced by other factors as noted above.

Figure 13 is the **extrapolated** temperature profile for hole 448 for depths below 6 m. The **MASBT** is $\approx -1.3^{\circ}\text{C}$. The extrapolated profile appears to be linear below ≈ 7 m. This suggests that the **interpretation** of the curvature in holes 433 and -439 as a change in sea bed temperature **may not** be tenable.

4b. Salt Concentration Measurements

Salt concentration **profiles** of the interstitial water in the subsea sediments were measured in two holes along our study line near the **Prudhoe** Bay West Dock (Fig. 9) using the sampling techniques described by Harrison and Osterkamp (1981). The salt concentrations were characterized by the electrical conductivity of the water samples measured in the laboratory at 25°C to a precision of $\approx 1/2\%$. The results are given in Table 2 and graphed in Fig. 14, 15, 16, 17. Hole 438S-1980 **and** hole 439-1981 were driven within a few meters of each other. There is a difference in depth to the ice-bonded permafrost table **of** ≈ 0.8 m with the latter hole being deeper. This difference could be explained by natural variability in the permafrost table **since** the holes were probably not exactly in the same location. In **addition**, the measured ice thickness (water depth) and **blow** counts for the last **interval** above the permafrost table were **different** for the two holes. Freeboard variations could also have been different for the *two* years. The differences in the **near-surface salt** concentrations between 1980 and 1981 may be associated with seasonal ice **formation** in the sea bed.

Evidence was **found** last year, in the **salt** concentration profiles, **for** a thin boundary layer just above the permafrost **table** where the **salt** transport seems to change from a convective to a diffusive regime. Holes 439 and 419 both show similar effects. **Figures 16 and 17** are the electrical conductivity and blow count profiles graphed **at** an expanded **scale** to illustrate the variations **in salt** concentration and blow counts in the diffusive boundary layer above the permafrost **table**. These data suggest the boundary layer is on the order of ≈ 0.3 m in **thickness**.

The nature of this boundary layer has not been determined at **this** time, however, the blow count profiles in Fig. 16 and 17 suggest a gradual increase in ice-bonding through the layer. It is thought that ice-bonding does not exist at the top of the diffusive **layer** and increases with depth over the **thickness** of the layer.

4c, Interstitial Water Pressure Measurements

Methods

A key factor in the evolution of subsea permafrost, which under the Beaufort Sea of Alaska is thawing at negative temperatures, is the transport of salt from the ocean through the developing thawed layer beneath the sea bed and into the ice-bonded permafrost below. In the relatively **coarse-grained** sediments at **Prudhoe** Bay, the rapid thaw rates indicated by probing and phase boundary data, together with theory, suggest that the salt necessary for this thawing is transported by gravity-driven convection of the interstitial water

(Harrison and Osterkamp, 1978). More direct evidence for this process comes from the measured interstitial water salinity distribution through the thawed layer. A thin boundary layer seems to mark a transition from a convective to a diffusive salt transport regime a few hundred mm above the impermeable ice-bearing permafrost table or "phase" boundary. The convective interstitial water velocity is thought to be small enough, a few hundred mm per year, that the heat transport regime is primarily conductive.

Although the previous evidence for the existence of convection is fairly convincing, more direct observations of it are desirable, particularly ones that can shed some light on the details of the "velocity field. The measurement of pressure gradients associated with the motion has this potential.

The pressure measurements were carried out in one hole along the line originating from North Prudhoe Bay State #1 well and bearing seaward about N 31° E, an area studied by several investigators since 1975. Pressure was measured in hole 438-1981, (438 m offshore and roughly 440 m from markers onshore near the edge of the tundra). The thawed layer thickness at this site is ≈ 14 m. The late May, 1981 sea ice thickness here was about 1.54-1.67 m, and extended to the sea bed. However, good hydraulic connection with the ocean still existed via a slushy layer at or near the bottom, because holes drilled through the sea ice rapidly filled with water. There was some evidence for several tens of mm of more solid ice under the slushy layer; this introduced some uncertainty as to the exact position of the sea bed. During the 4 day period of day-time observation

the tide did not float the ice at this site, but this sometimes occurs where the ice is in contact with the sea bed.

Following unsatisfactory results in the two previous years with a standpipe piezometer, a commercially available pneumatic pressure transducer (Sinco model 51481 with model 51411A readout) was used in 1981. The transducer was mounted inside a piece of A-rod, and connected to the probe assembly of the University of Alaska interstitial water sampling equipment (Harrison and Osterkamp, 1981) with a short piece of rubber tubing. The probe assembly contains a filter through which the transducer couples to the interstitial water. The tubing and probe assembly were completely filled with antifreeze, and the A-rod driven into the sea bed sediments using portable driving equipment. Pressure was read sequentially at increasing depths down to the ice-bonded phase boundary. Tide was determined concurrently by measuring the water level in a borehole through the sea ice. This water level was measured with respect to a mark on an adjacent string of A-rod, driven about 7.6 m into the sea bed to provide a stable reference.

Temperature and electrical conductivity of the interstitial water were determined in hole 439, 1 m seaward of the side of the pressure measurements, using already described techniques (Osterkamp and Harrison, 1981; Harrison and Osterkamp, 1981).

Results

The results of the pressure measurements are given in the first 4 columns of Table 3; tide data are incorporated in column 3 and are

shown graphically in Figure 18. The system **resolution** is about 0.07 kN/m^2 (7 mm head) and the nominal linearity is about 0.1%. There is a zero uncertainty of $< 2.1 \text{ kN/m}^2$ (0.21 m head); the correct zero was determined in the course of the measurements to an uncertainty of 0.3 kN/m^2 (30 mm head). Tide measurement and interpolation had an uncertainty of several mm. The expected resolution was obtained only on the last of the 4 days (May 27 to May 30, 1981) required to make the **measurements**. Resolution or stability, seemed to be poorer on the first two days, sometimes up to 5 times larger than expected. It is uncertain whether the cause was instrumental and/or operator error, or whether conditions in the sediments were actually fluctuating in a way that was not related simply to tide.

Independent of this uncertainty, the driving of the **piezometer** introduced a marked pressure transient at the shallower depths; the pressures in Table 3 are the equilibrium values. At depths 0.235, 0.540 and 0.844m below sea bed the pressure, **p**, closely followed the simple time **behaviour** (Figures 19 and 20),

$$P = P_{\infty} + P_t e^{-t/\tau}$$

where P_{∞} is the equilibrium value, P_t is the transient pressure amplitude, and τ is the time constant of the transient pressure amplitude.

At the 0.844m depth where τ was large, the pressure was first observed to increase over a period of several minutes, after which the above **behaviour** was closely followed. At depths of 3.283 m and greater, any transient **behaviour** was too rapid to be observed. A summary of the transient **behaviour** is given in Table 4. If there are no **complications** due to freezing, the time constant τ is most obviously

related to the decay time for the pressure introduced by driving the **finite** volume **piezometer** (41.3 mm diameter). Hydraulic conductivity is sometimes estimated this way. The response at small time **in Figure 20** may represent the **inflow** time of **the** small but finite (< 20 mm³) volume of water **required to** displace the transducer diaphragm.

As noted, tidal corrections are included in column 3 of Table 3. These greatly smooth the variation of pressure with depth as measured on May 30, they slightly smooth the May 29 data, and **it** is uncertain whether there is any smoothing on the previous two days. Evidently the interstitial water responds closely to tidal-induced pressure variation, at **least** at depths below about 5 m.

To **interpret** the measured pressures in terms of interstitial water flow, it is necessary to compute the hydrostatic pressure. This can be done because the interstitial water electrical **conductivity** and temperature data taken **in** the adjacent **hole** 439 permit density to be calculated with high accuracy. Hydrostatic pressure (P_{HS}) at depth (h) below water surface *is* then given by

$$P_{HS} = \int_0^h \rho g \, dh'$$

where g is the local gravitational acceleration. As an approximation **we** can neglect the **variation of** density and approximate P_{HS} by

$$P_{HS} \approx \rho_r g h$$

where ρ_r **is** some appropriate reference density. This is done in column 5 **of** Table 1, using $\rho_r = 1.0350 \text{ kg/m}^3$.

Figures 12 and 14 show the measured temperatures and electrical conductivity (salinity can be calculated from the latter), and Fig. 21

shows the resulting density distribution, as computed by oceanographic methods. It is not necessary to take into account the variation of temperature in this case, which causes a density variation on the order of only 1 part in 10^4 . The dotted line in Fig. 21 results from a particular salinity model above the depth that measurements were made. The temperature and salinity data indicate that ice may have been present in the top 1.45 m; if so, the temperature (which has to be extrapolated above 0.62 m) determines the salinity of the interstitial water by the requirement of phase equilibrium. The hydrostatic pressure, computed on the basis of Fig. 21 is shown in Fig. 22 and in column 7 of Table 3. For convenience, and to facilitate comparison with the simple $\rho_r gh$ model in column 5, the quantity $\int \rho g dh' - \rho_r gh$ is shown. The difference is small, and it will be seen that the simpler model of hydrostatic pressure is adequate.

The difference between measured and hydrostatic pressure is given in Figure 23 and in column 8 of Table 3. The same quantity using the simple $\rho_r gh$ model (column 6) is basically the same, the main difference being an insignificant (from the point of view of the observation) shift in the zero of the abscissa of Fig. 23. The bar above this zero represents its uncertainty, which has contributions from uncertainty in instrumental zero and in the density of the sea water in the hole made for tide measurements. The point marked "Freezing?" was taken after the piezometer had been at the phase boundary for 34 minutes. Its high value is probably a result of freezing in or around the piezometer, and therefore is not an undisturbed in situ value. The parentheses around the point at depth

0.844 m **indicate** that equilibrium had probably not been achieved when pressure was last recorded at **the** end of the day, May 27.

The solid straight **line** below **5.721 m** in Fig. 23 is the result of a least squares fit to the **data**, taken on May 30 when, as noted, stability and the **full** resolution were obtained. The dotted line **is** the projection to the sea bed. The slope is -0.16 kN/m^3 , or in terms of head, -0.016 m/m . This non-zero **slope** is a striking feature of Fig. 23, and a key point requiring **discussion** of whether it is real or not. This apparent slope could be caused by an instrumental nonlinearity of 1%. The nominal **linearity** is 0.1%, but no check was made. The slope could also be caused by a systematic error in depth that **would** result from tilt in the drill rod from the vertical. A **tilt** of about 10° would **be** necessary **to** explain a slope of this magnitude. This seems large, but not impossible. It is **felt** that the non-zero slope is probably a real effect, though final judgement cannot be made without an instrument linearity check and a tilt measurement.

Interpretation

Although some of the structure evident **in** Fig. 23 above 4 m depth may be due to instrumental problems or changing conditions, as noted earlier, most of it appears to be real. A question is **how** much of it might be due to the presence of **ice**. There is normally some seasonal **ice** formation beneath the sea bed **in** this location, as already discussed, but the ice-bearing layer was no thicker than about **1.45** m at the time of pressure measurement. Possibly the high

values of the shallowest 3 points beneath the sea bed in Fig. 23 could be related to seasonal ice formation. The pressure transients summarized in Table 3 evidently occur both within and below this seasonally ice-bearing layer.

The non-zero slopes in Fig. 23 indicate interstitial water motion with a vertical component. This component, which follows the gradient in Fig. 23 seems to change direction in a complex pattern above 4 m; probably more complex than indicated by the few data points. In the shallow ice-bearing layer the permeability and hence the motion, may be small even though the gradients are large. A striking feature is the non-zero slope of the straight line fitted to the May 30 data (5.721 m and below), which, as discussed previously, is probably a real effect. If so, it indicates a predominantly downward flow of the interstitial water in this depth range. It is tempting to interpret the fine structure as well. For example, the slope appears to be generally zero between 5 and 9 1/2 m, which would indicate a very small component of vertical motion in this particular depth range. However, this may be because the standard deviation of the points from the solid line is only 0.10 kN/m², which is the same order as the instrumental resolution of 0.07 kN/m².

An estimate of the magnitude of the vertical velocity can be made from Darcy's law and hydraulic conductivity data. From Darcy's law

$$\frac{v_y}{K} = -\frac{\partial}{\partial y} (p-p_{H.S.})$$

where v_y is the vertical component of the filtration velocity (velocity times porosity), K is the hydraulic conductivity, and y is positive downward. The right side is the negative of the slope of the

line in Fig. 23, (0.016 m/m). The filtration velocity corresponding to the observed hydraulic conductivity here (1 to 10 m a⁻¹) is therefore between 0.016 and 0.16 m a⁻¹. For a porosity of 0.4, the water velocity would be between 0.04 and 0.4 m a⁻¹. Uncertainty in the porosity and in the true value for the slope in Fig. 23 increase this uncertainty range and velocity magnitude and direction must vary in space and probably in time. Nevertheless, this velocity estimate from pressure data is consistent with those made by two independent methods employing temperature, electrical conductivity, and phase boundary data, as noted earlier. If not more accurate, the present estimate is more satisfactory, since pressure is more directly related to flow.

The gradient in Fig. 23 is positive near the sea bed but water does not seem to be entering there even though the deeper velocity is downward. A pattern of convection that is complex, at least in the upper 4 m of sediments, is therefore suggested by the observations. The situation may change seasonally with the elimination of ice from the shallow sediments, which should greatly increase the hydraulic conductivity there.

In a more conventional situation, data such as in Fig. 23 would be interpreted in terms of soil consolidation. This could possibly be occurring at some depths above 4 m, but at most depths it is masked by some other effect, since the water motion following the gradient in Fig. 23, is down over much of the depth range, while in a simple consolidation situation it should be up. The dominating effect is probably the gravity driven convection which occurs to

deliver salt to the thawing phase boundary interface. Rough estimates of the interstitial water velocity that might be associated with consolidation suggest that it should be an order of magnitude less than that associated with convection.

Summary ?

Interstitial water pressure and density were measured in the thawed layer overlying ice-bearing subsea sediments under Prudhoe Bay, Alaska, at a site where the thawed layer is ≈ 14 m thick. Convective motion of the interstitial water is indicated by these, as well as by other, independent, observations. At this site the pattern of motion is complex in the top 4 m of sediment. The vertical component is up at the sea bed, but probably reverses several times between there and the 4 m depth. An average downward flow seems to exist below 4 m, subject to some restrictions on observational accuracy. In this depth range, an order of magnitude of the vertical component of between 0.04 and 0.4 m a^{-1} is suggested.

4d. Phase Boundary Characteristics

The position of the phase boundary was determined from driving data obtained when the temperature probes and interstitial water sampling probes were driven through the thawed sediments. Blow count profiles for holes 419 and 439 are shown in Fig. 24 and 25 and also in Fig. 16 and 17. Because of an uncertainty in the water depth, the depths in Fig. 16, 17, 24 and 25 are uncertain by about 10 cm. These profiles suggest that the phase boundary is

diffuse with a thickness of several tenths meter. Figure 26 is a graph of the position of the phase boundary with distance offshore for a number of holes, including several from past years. These data show that the phase boundary increases linearly with distance offshore between holes 398 and 448. If it is assumed that the shoreline erosion rate was 1 m a⁻¹ then the distance between these holes represents a time of 50 years. Figures 14 and 15 show that there is no appreciable change in the salt concentration profiles between holes 419 and 439. It is concluded that the interstitial water velocity must be at least 0.25 m a⁻¹ for the salt concentrations to keep up with the moving phase boundary. This minimum interstitial water velocity is at the high end of the range of velocities estimated from the pressure and temperature data.

Phase boundary temperatures can be estimated from the measured temperature profiles in holes 418, 433, 439 and 448. The values obtained depend on the method used to make the estimate. Judging from the return of the temperatures in these holes to equilibrium and the thermal gradients near the bottom of the hole it appears that the phase boundary temperatures should be 0.02-0.04°C colder than the last measured bottom-hole temperature. According to this estimate, the phase boundary temperatures are; hole 418, -2.42°C; hole 433, -2.33°C; hole 439, -2.38°C; hole 448, -2.40°C. Generally, these phase boundary temperatures have been close to -2.40°C in other holes along this study line in past years.

The salt concentration of the interstitial water (as characterized by the electrical conductivity) at the phase boundary

differe**d** **slightly** between hole 419 (6.117 S-m⁻¹) and hole 439 (6.206 S-in-l). Some of this difference could be related to the fact that the **water** samples are obtained somewhat above the phase boundary-because of the placement of the holes in the probe. Also, spatial **variability** in the phase boundary salt concentration cannot be ruled out at present.

c. Barrier Islands

Thetis **Island**

A hole was drilled **on July 29, 1980** using a rotary-jet drilling rig (Osterkamp and Harrison, 1981) at a site **midway** between the **cabin** and the SE end of **the island** and 31 m from the western shore. Total depth reached was **≈ 29 m**. The first temperature log was measured immediately **after drilling** and suggests ice-bonding down to the 15-16 m depth, except for a thawed surface layer, with possible intermittent ice-bearing or ice-bonded sediments below this depth. Figure 27 shows the temperature log obtained a year later. This log also shows what appears to be ice-bonded sediments down to 16-17 m **with** a nearly **uniform** temperature profile **below** this depth. There is some remaining thermal disturbance judging from the **unevenness** of the profile and the data point at 24 m. A preliminary **interpretation** of this temperature profile suggests that **it** is a result of the motion of the island over the present hole site sometime during the past century.

Reindeer Island

A temperature profile measured in hole D on Reindeer Island is shown in Fig. 28. This hole was drilled on August 31, 1979 at a site \approx 300 m, N 250° E from the USGS tower and \approx 4 m from shore. It appears that the hole has not yet reached thermal equilibrium and that there are strong variations in thermal properties with depth or surface temperature with time (on a long-term basis). Since the hole is so close to the shore, the last possibility seems likely.

Cross Island

Figure 29 is a temperature profile measured on June 2, 1981 in a hole drilled on Cross Island on July 23, 1980 at a site N 294° E from the USGS tower and \approx 103 m from the southern shore. Unfortunately, this hole is located a few meters from a small pond which makes the profile difficult to interpret.

Flaxman Island

A hole was drilled to the \approx 10 m depth on Flaxman Island at a site N 118° E from the exploration well and 213 m north of the shoreline on July 28, 1980. It was not possible to log this hole in 1981 because of a gas flow from the pipe. Some of this gas was collected and analyzed for isotopic composition by K. Kvenvolden (USGS). The isotopic composition relative to a PDB standard was -91.6 for one bottle of gas and -80.4 for another. Such compositions indicate that the gas was biologically generated.

Portable drilling and probing methods were used to study subsea permafrost beneath the **Chukchi** and Beaufort Seas. Data were obtained on the temperature and chemical (salt) regimes including information on the depth to ice-bearing permafrost and the nature of the phase boundary. A profile of the **pressure** of the interstitial water in the thawed subsea sediments was obtained - the first measurements of these kind reported for subsea permafrost. The results are summarized on a regional basis below.

A. **Chukchi** Sea

Rock was encountered at or near the sea bed in the area along the **Chukchi** Sea coast between Peard Bay and **Ogotoruk** Creek. Since this rock may contain segregated ice, it cannot be assumed to be a good foundation material for bottom-founded structures. Severe problems may be encountered when laying pipelines in this rock.

Our data base is not sufficient to assess the occurrence or distribution of this subsea permafrost consisting of rock and possibly segregated ice. Additional research is needed to determine the occurrence and distribution of subsea permafrost in the **Chukchi** Sea and to determine if the rock permafrost contains segregated ice.

B. Beaufort Sea

1. Harrison Bay and the Area to the West

Holes were drilled to the NW of Cape **Halkett**, NE of **Atigaru** Point and N of Thetis Island. Data from these holes suggest that

ice-bearing permafrost exists close to the sea bed, in relatively deep water far from shore. This suggests that **there will** be substantial problems for bottom-founded structures and pipelines *in these* areas. At present, our data base is too sparse to further assess the hazards of **subsea** permafrost for **OCS** development in these areas.

2. Prudhoe Bay - West Dock

Additional studies, funded by NSF, were conducted to determine the nature **of** the heat and salt transport processes in the thawed subsea sediments along our previous study line near the West Dock. This work will eventually **help** us to extrapolate our sparse data base **to other** areas.

Temperature profiles **along** this line at holes 433 and 439 suggest that the interstitial water is moving downward with a velocity of a few tenths m a^{-1} . This contrasts with a similar but upward movement found near the hole 439 site in **1980**. It is thought that this water movement is part of a density-driven convection system in the subsea sediments. This interpretation is supported by the salt concentration profiles and by pressure measurements. The salt concentration profiles suggest that interstitial water is moving downwards through the thawed sediments. Just above the phase boundary the salt transport appears to be diffusive. The phase boundary is a few tenths meters in thickness with a phase boundary temperature of about **-2.3 to -2.4°C**. Movement of the phase boundary between holes 398 and 448 suggests that the minimum water velocity is 0.25 m a^{-1} . The pressure measurements at hole 438 show that the pattern of water motion is complex in the top 4 m of

sediment. The vertical component is up **at the** sea bed, but probably reverses several times between **there** and the 4 m depth. An average downward flow seems to **exist** below 4 m, In this depth range, a rough estimate **of** the vertical component of water velocity is between 0.04 and 0.4 m a⁻¹.

The salt concentrations near the sea bed, down to 4-5 m, in holes 419 and 439 are much lower than expected from data obtained in previous years. This suggests that the sea bed was not frozen at the site or that it contained less ice than in past years.

Temperature profiles and drilling information from the barrier islands (Thetis, Cross and Reindeer Islands) suggest movement of these islands in recent times. Permafrost exists beneath these islands but with a very complex ice-bearing *or* ice-bonded structure. Gas of a **biogenic** origin was found on **Flaxman** Island in a shallow **borehole**.

x. ACKNOWLEDGEMENTS

We wish to acknowledge the assistance of Robert Fisk in all phases of this research including work under difficult to impossible field situations, the NOAA helicopter crews and the Geophysical Institute machine shop personnel. Logistical support was provided **by OCSEAP**. The National Science Foundation supported parts of this research under **NSF** grant **DPP 77-28451**.

REFERENCES

- Harrison, **W. D.** and **Osterkamp**, T. E., 1981. A probe method for **soil** water sampling and subsurface measurements. *Water Resources Research*, Vol. **17**, No. 6, p. 1731-1736.
- Harrison, **W. D.** and **Osterkamp**, T. E., 1978. Heat and mass transport processes in **subsea** permafrost I. ? An analysis of molecular diffusion and its consequences. *Journal of Geophysical Research*, Vol. 83, No. C9, p. 4707-4712.
- Osterkamp, T. E. and Harrison, **W. D.**, 1981. Methods and equipment for temperature measurements in subsea permafrost. Geophysical Institute Report **UAGR-285**, Geophysical Institute, University of Alaska, Fairbanks, Alaska 99701.
- Osterkamp**, T. E. and Harrison, **W. D.**, 1980. Subsea permafrost: Probing, thermal regime and data analysis. **Annual** Report to **BLM-NOAA, OCSEAP**, Arctic Project Office, University of Alaska, Fairbanks, Alaska.

FIGURES

- Figure 1.** Map showing approximate hole locations in the Cape **Lisbourne-Point** Lay area of the **Chukchi** Sea.
- Figure 2 .** Map showing the approximate location of the **Ogotoruk** Creek hole in the **Chukchi** Sea.
- Figure 3. Map showing the approximate locations of the **Esook** holes (A, B, C), **Atigaru** Point hole and the Thetis holes (A,B) in the Harrison Bay area of the Beaufort Sea.
- Figure 4. Measured temperature profile in **Esook** hole A on May 29, 1981.
- Figure 5. Measured temperature profile in **Esook** hole B on May 29, 1981.
- Figure 6.** Measured temperature profile in the **Atigaru** Point hole on May 21, 1981.
- Figure 7. A temperature profile in the **Atigaru** Point hole on May 28, 1981 which was measured immediately after the **borehole** was heated.
- Figure 8.** Measured temperature profile in Thetis **hole** B on May 29, 1981.
- Figure 9. Map showing the locations of the Prudhoe Bay - **West** Dock holes 398, 418, 419, 433, 438, 439 and 448.
- Figure 10. Measured temperature profile in the **Prudhoe** Bay - West Dock **hole 418** on June 2, 1981. .
- Figure 11. Measured temperature profile in the Prudhoe Bay - West Dock hole 433 on June 2. 1981.

Figure 12. Measured temperature profile in the Prudhoe Bay - West Dock hole 439 on June 2, 1981.

Figure 13. Extrapolated temperature profile for the Prudhoe Bay - West Dock hole 448 for depths below 6 m.

Figure 14. Measured salt concentration (electrical conductivity) profiles in the Prudhoe Bay - West Dock holes 438S-1980 and 439-1981.

Figure 15. Measured salt concentration (electrical conductivity) profile in the Prudhoe Bay - West Dock hole 419 at the end of May, 1981.

Figure 16. Expanded **scale** profiles for salt concentration and blow count near the phase boundary in the Prudhoe Bay - West Dock hole 439.

Figure 17. Expanded scale profiles for salt concentration and blow count near the phase boundary in the Prudhoe Bay - West Dock hole 419.

Figure 18. Tide data, May, 1981, for our study site (hole 438) on the Prudhoe Bay - West Dock line.

Figure 19. Transient pressure response and its logarithm for 0.235m depth. The line through the latter points is drawn by eye, and its **intercept** and slope used to find the transient pressure amplitude (P_t) and time constant, τ . The exponential curve is calculated using these values.

Figure 20. Transient pressure response for 0.844m depth. See Figure 2 for details.

- Figure 21. Specific gravity of interstitial water as a function of depth. The variation of temperature has not been included because it is small, on the order of 1 part in 10^4 .
- Figure 22. Hydrostatic pressure minus hydrostatic pressure at constant specific gravity (1.0350) as based on Figure 21. It "does not include the **variation** of temperature, which would have an effect on the order of 1 part in 10^3 .
- Figure 23. Pressure measurements minus hydrostatic pressure. Data were taken on 4 days, May 27 to 30, 1981. Lines join points taken the same day.
- Figure 24. Blow count profile for hole 419.
- Figure 25. Blow count profile for hole 439.
- Figure 26. Depth to the ice-bonded permafrost **table** (phase boundary) versus distance offshore for several **holes** along our study line at Prudhoe Bay - **West Dock**.
- Figure 27. Pleasured temperature profile in the Thetis Island hole on July 28, **1981**; one year after the **hole** was drilled.
- Figure 28. Measured temperature profile in hole D on Reindeer Island on June 2, **1981**; \approx 9 months after the hole was drilled.
- Figure 29. Measured temperature profile in the Cross Island hole on June 2, 1981; \approx 10 months after the hole was drilled.



166

165 30

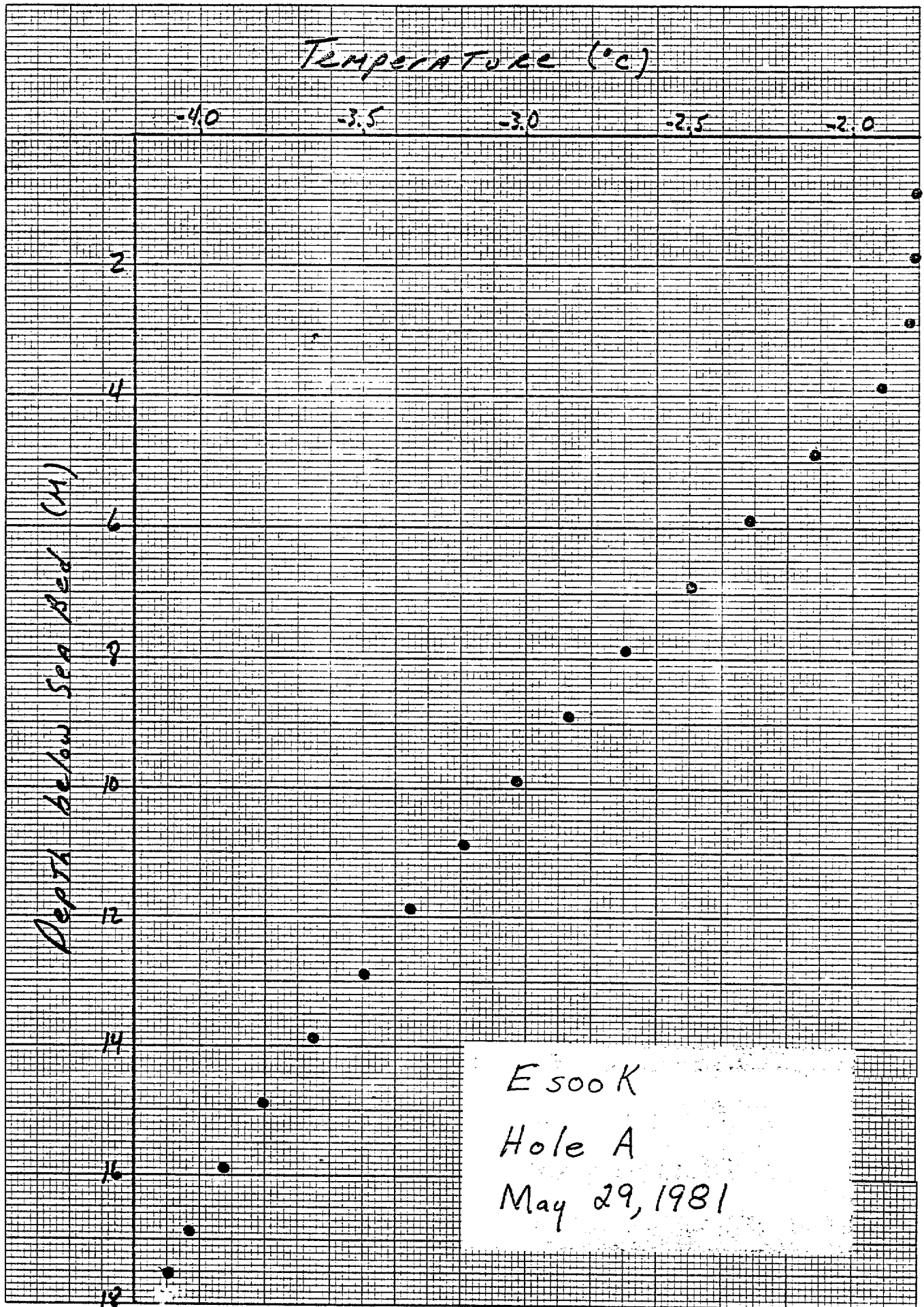
165 00

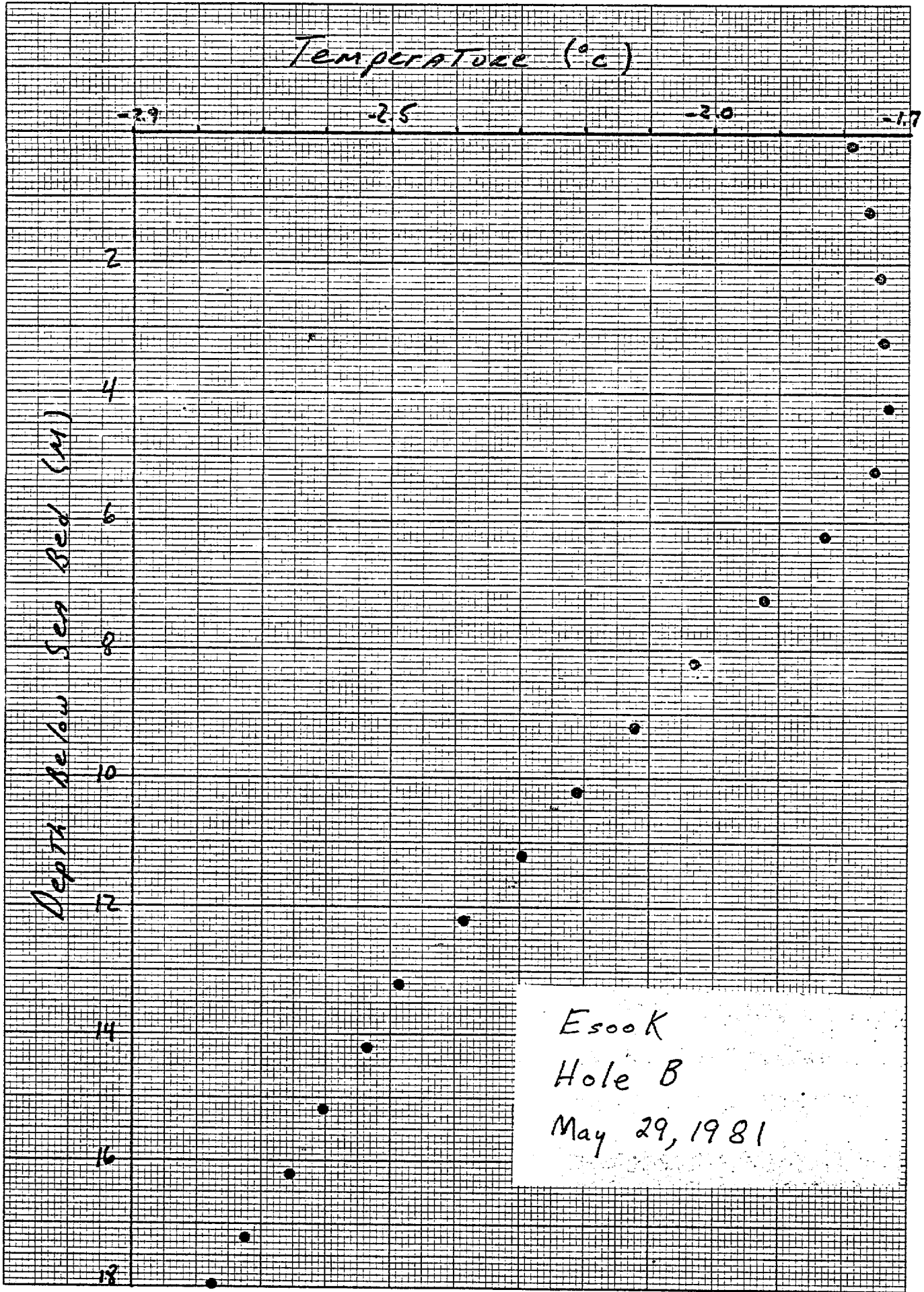
164 30

164 00

163 30

UNIT IS PRESENTED IN THE USUAL MANNER

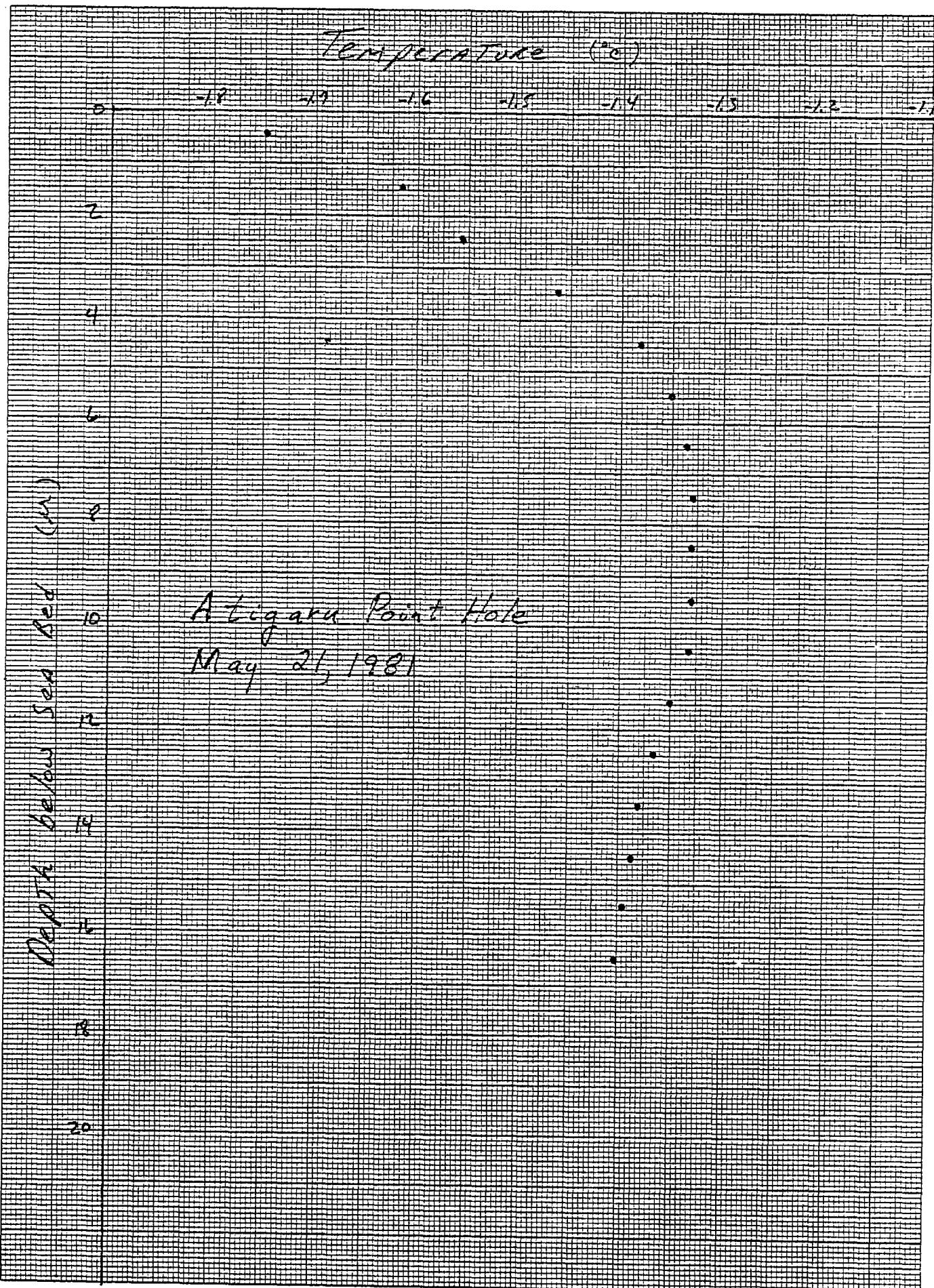




Esook
Hole B
May 29, 1981

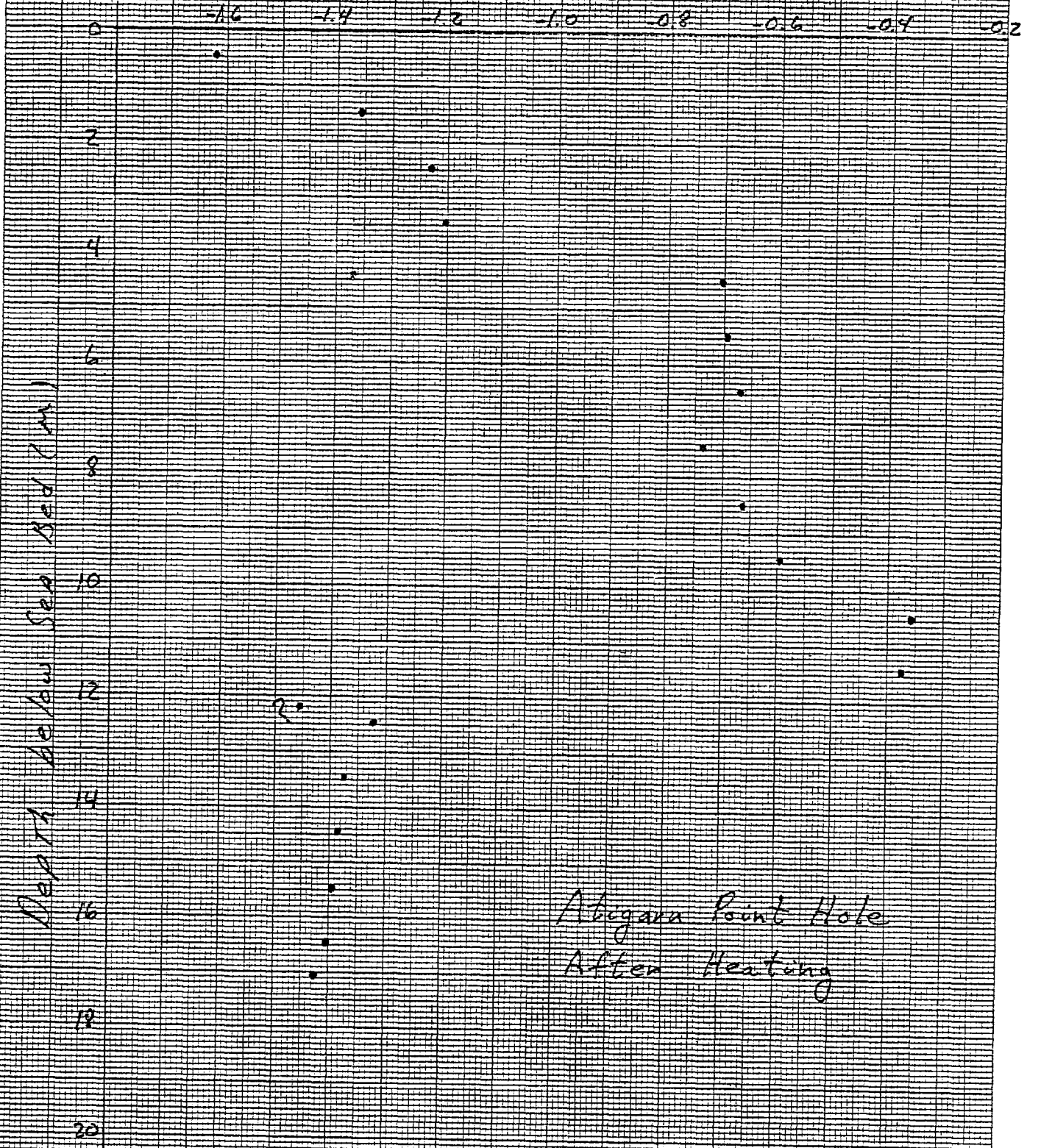
810521

Temperature (°C)



Atigara Point Hole
May 21, 1981

TEMPERATURE (°C)

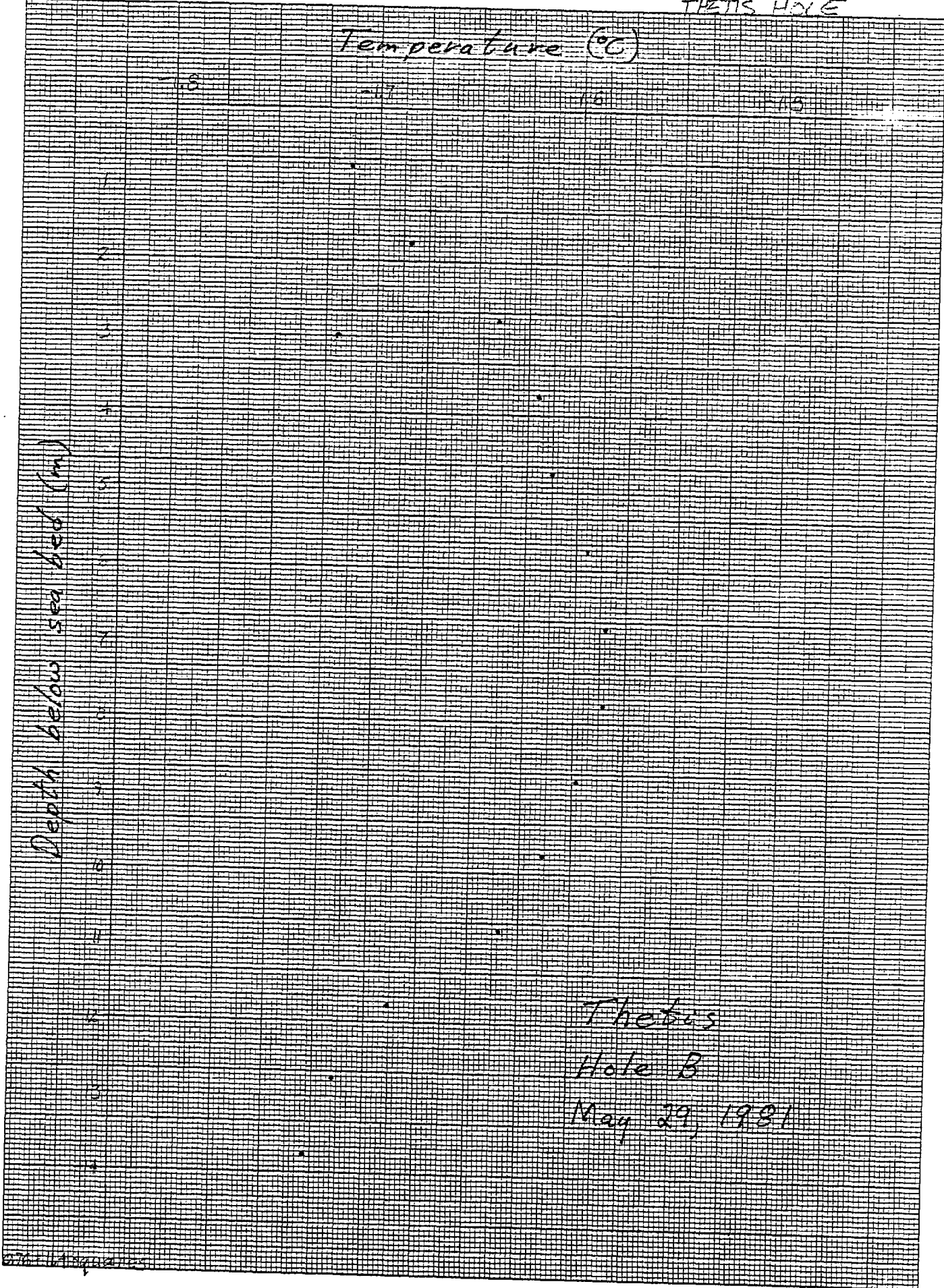


Atigara Point Hole
After Heating

THEBIS HOLE

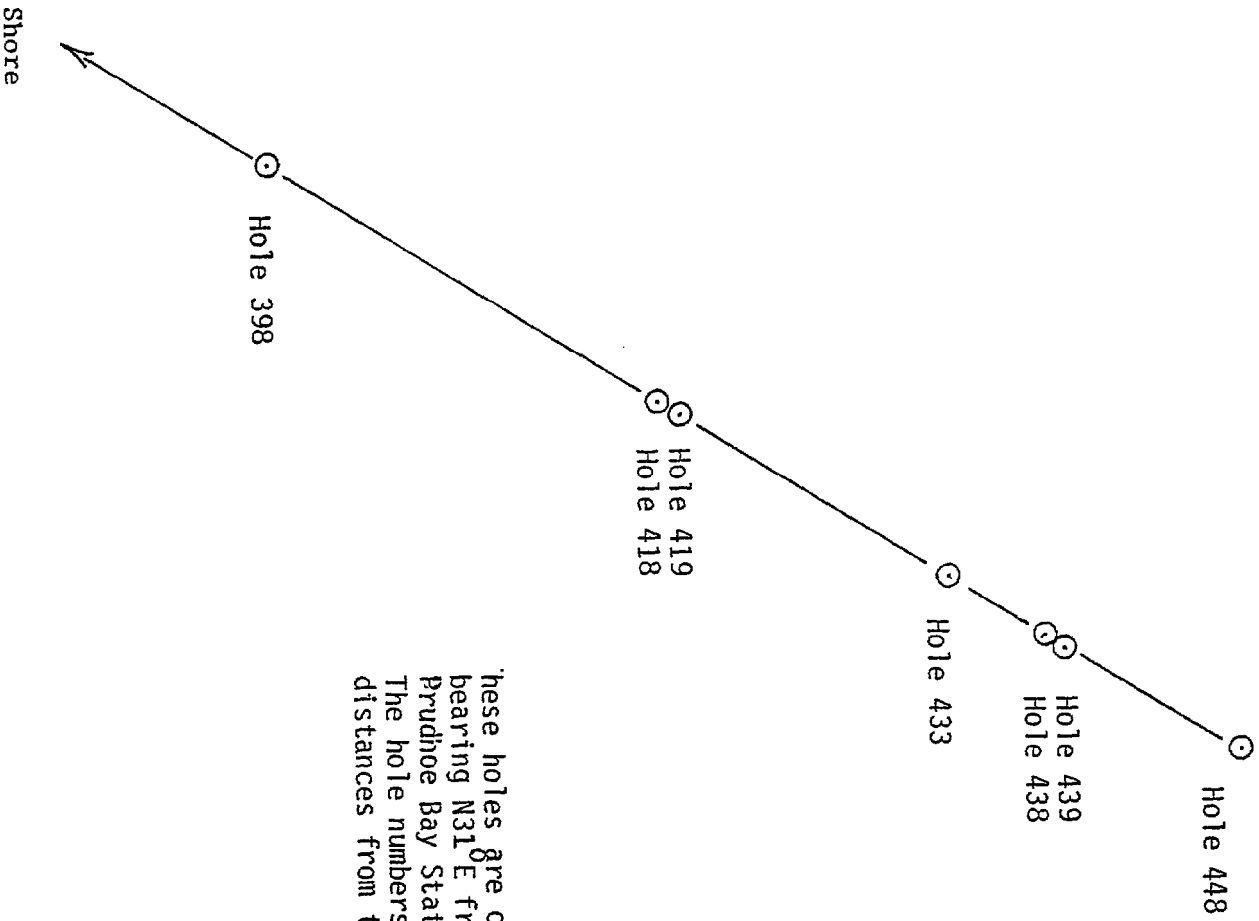
Temperature (°C)

Depth below sea bed (m)



Thebis
Hole B
May 29, 1981

N



These holes are on a line bearing N31°E from North Prudhoe Bay State #1 well. The hole numbers represent distances from the shore.

DEPTH BELOW SEA LEVEL (m)

20

20

20

20

10

0

10

20

30

40

50

60

PRUDHOE BAY

HOLE 418

JUNE 22, 1951

Temperature (°C)

Depth below sea bed (m)

-2.3 -2.2 -2.1 -2.0 -1.9 -1.8

2

4

6

8

10

12

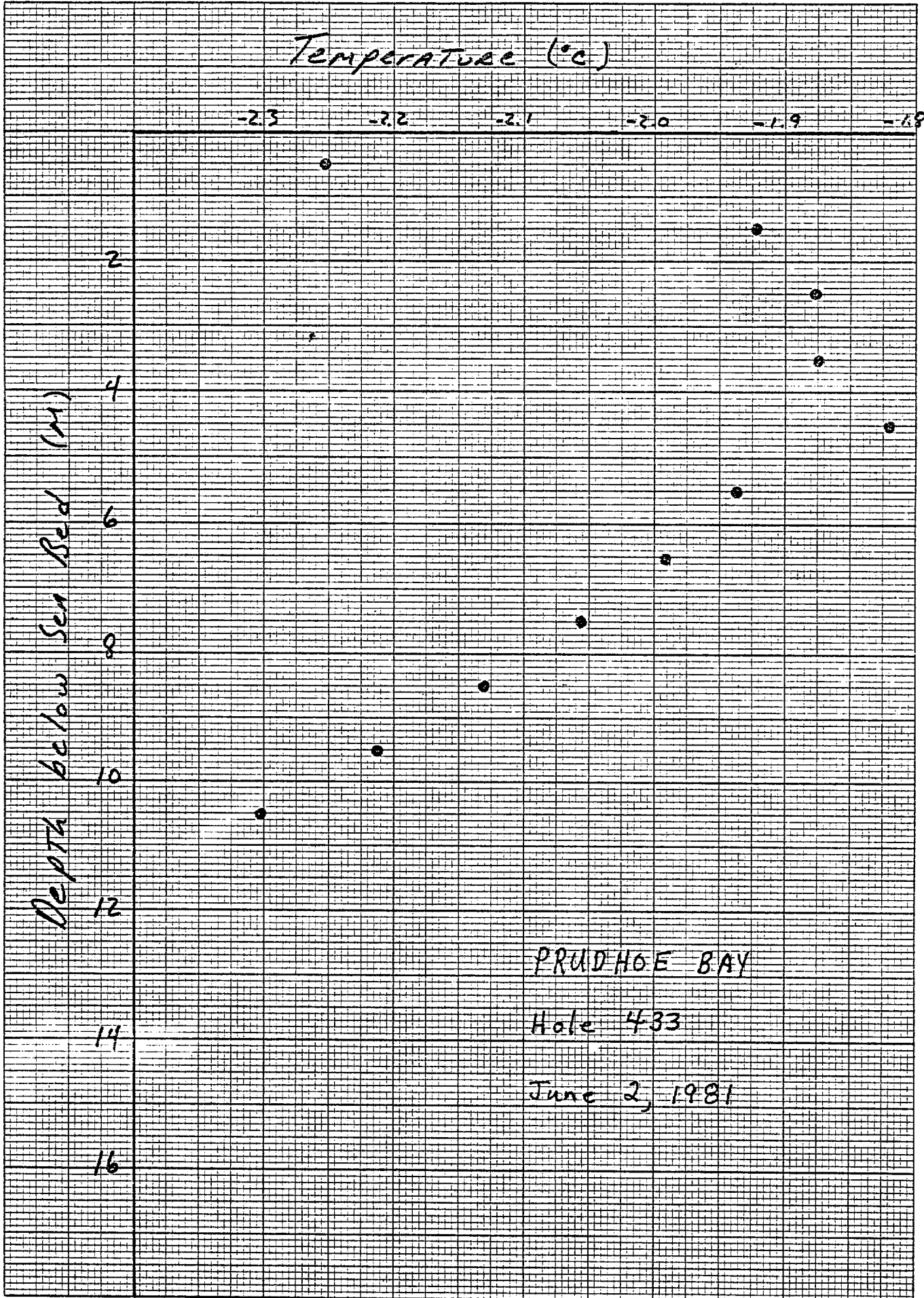
14

16

PRUDHOE BAY

Hole 433

June 2, 1981



TU 4314

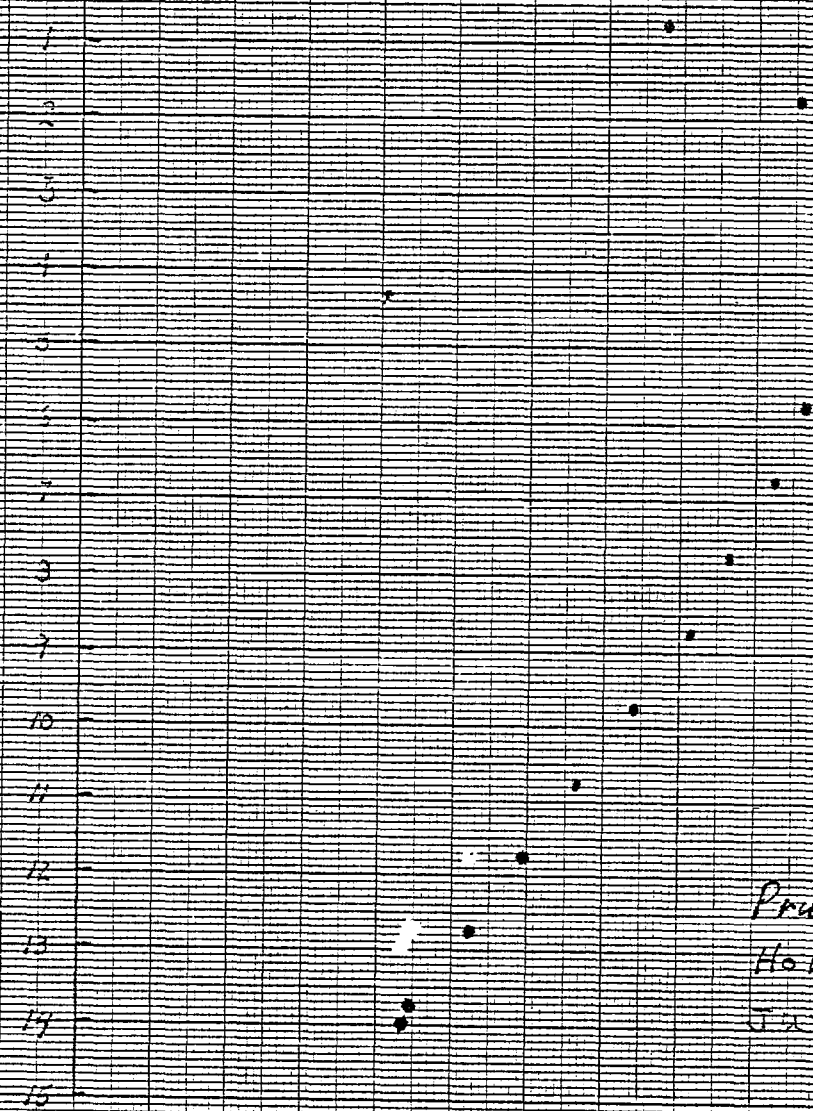
NEUFEL & ESSEN CO. MADE IN U.S.A.

DEPTH BELOW SLASHED (FTH)

5
7
9
11
13
15

TEMPERATURE (F)

20.5 20.5 20.5



Prudhoe Bay - West Dock
Hole 439
JUL 02 1971

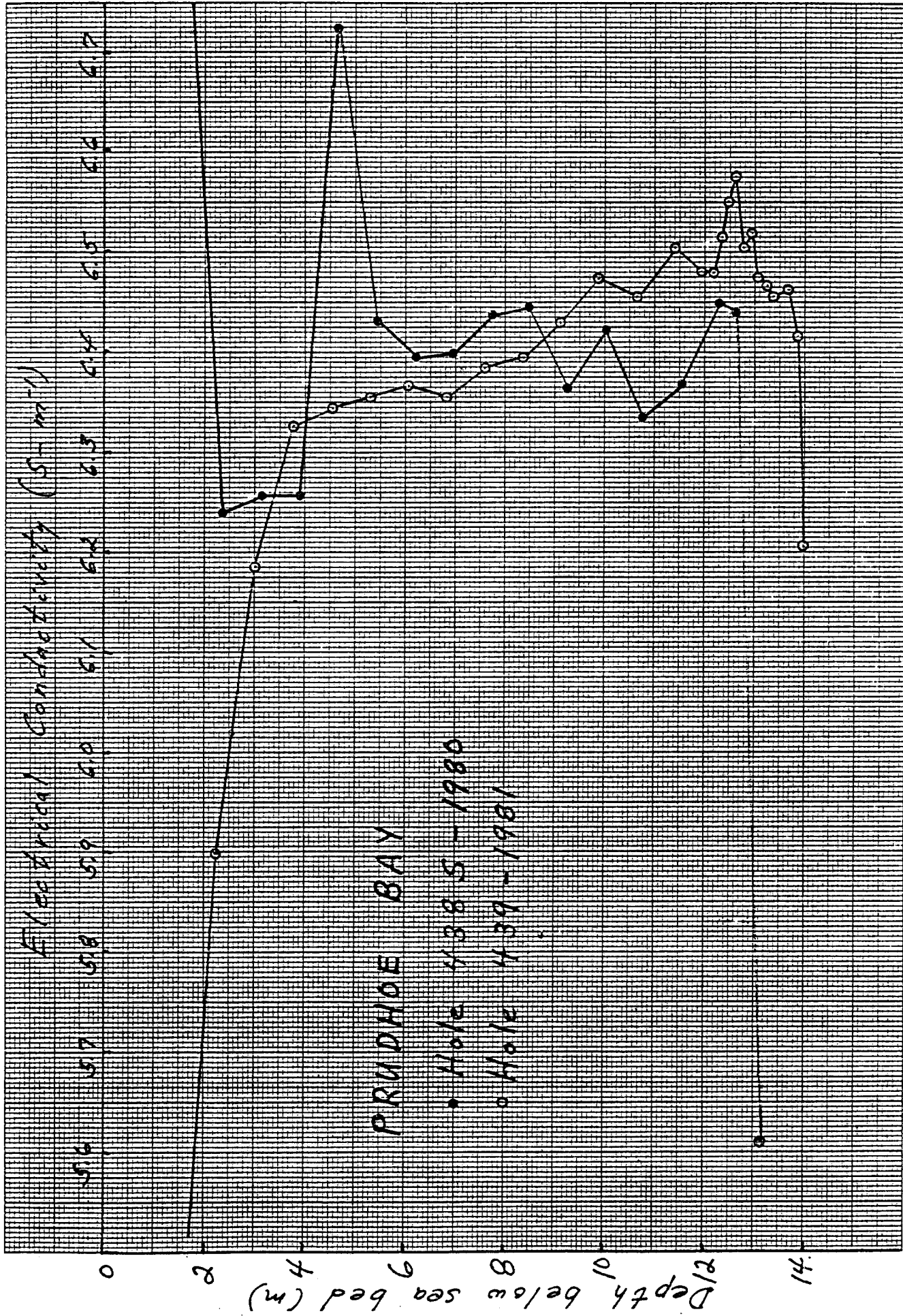
Depth below sea bed (m)

Temperature (°C)

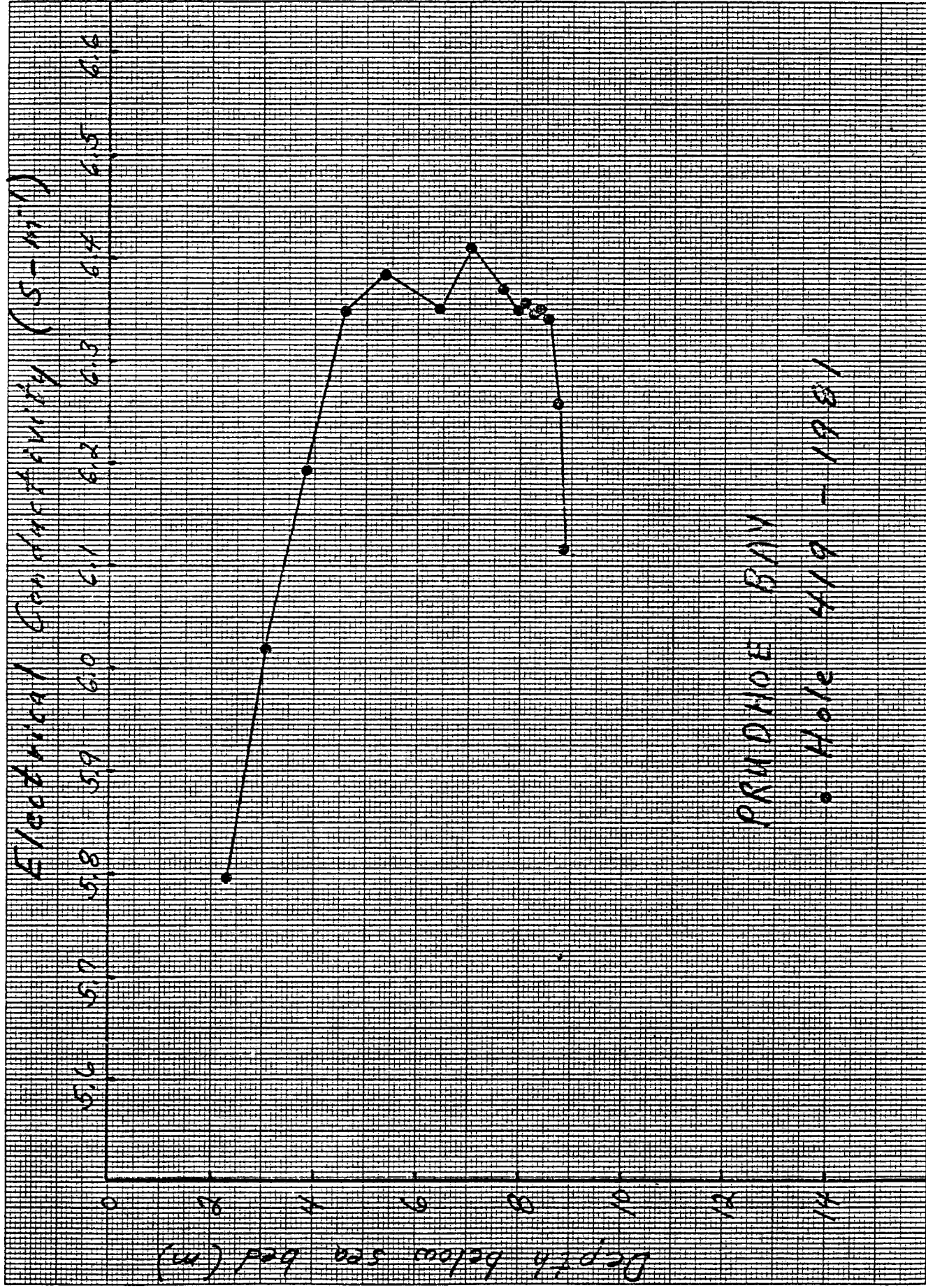
46 1512

Paradise Bay - West Dock
Extrapolated profile
Hole 448

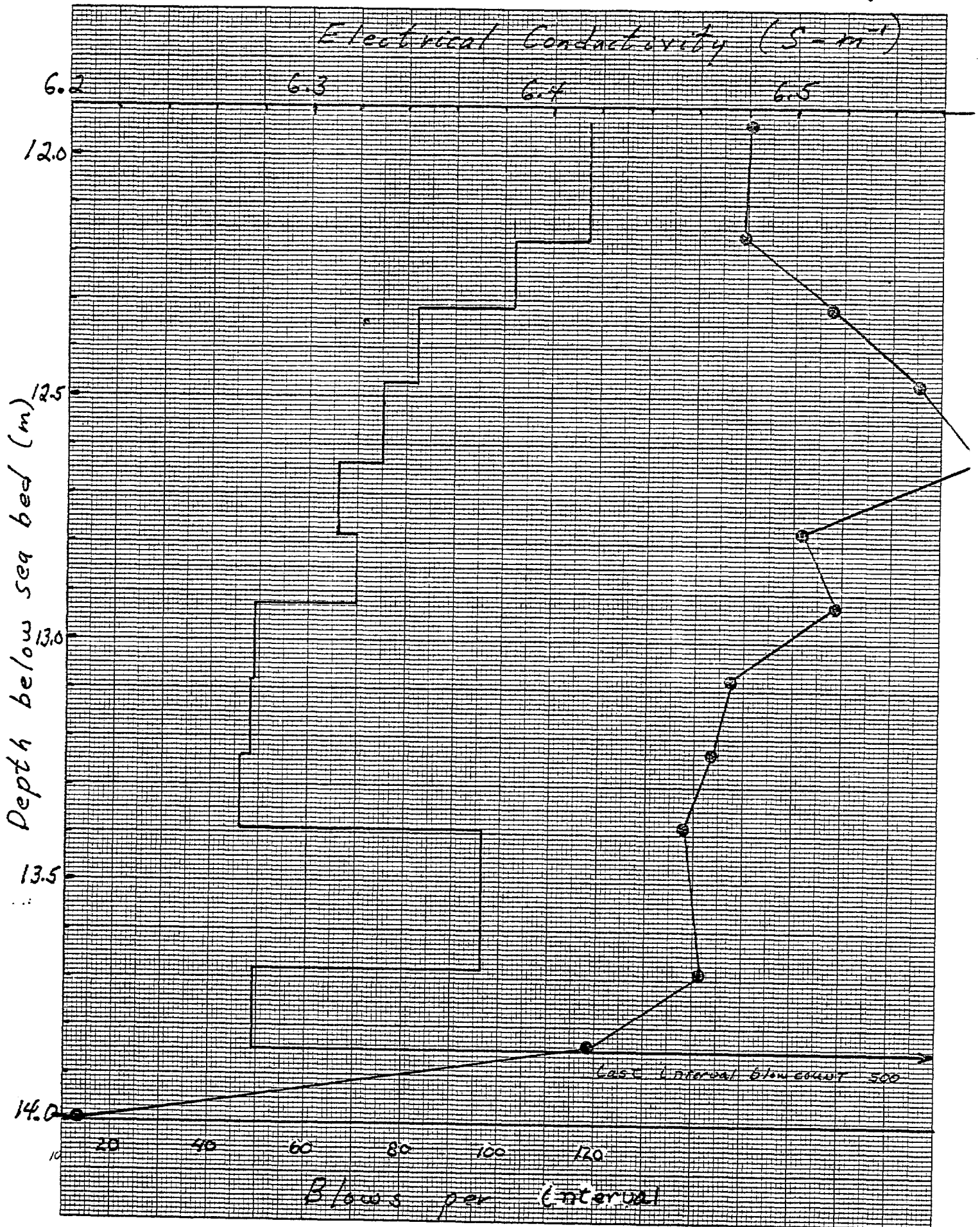
HOLE 448
810528

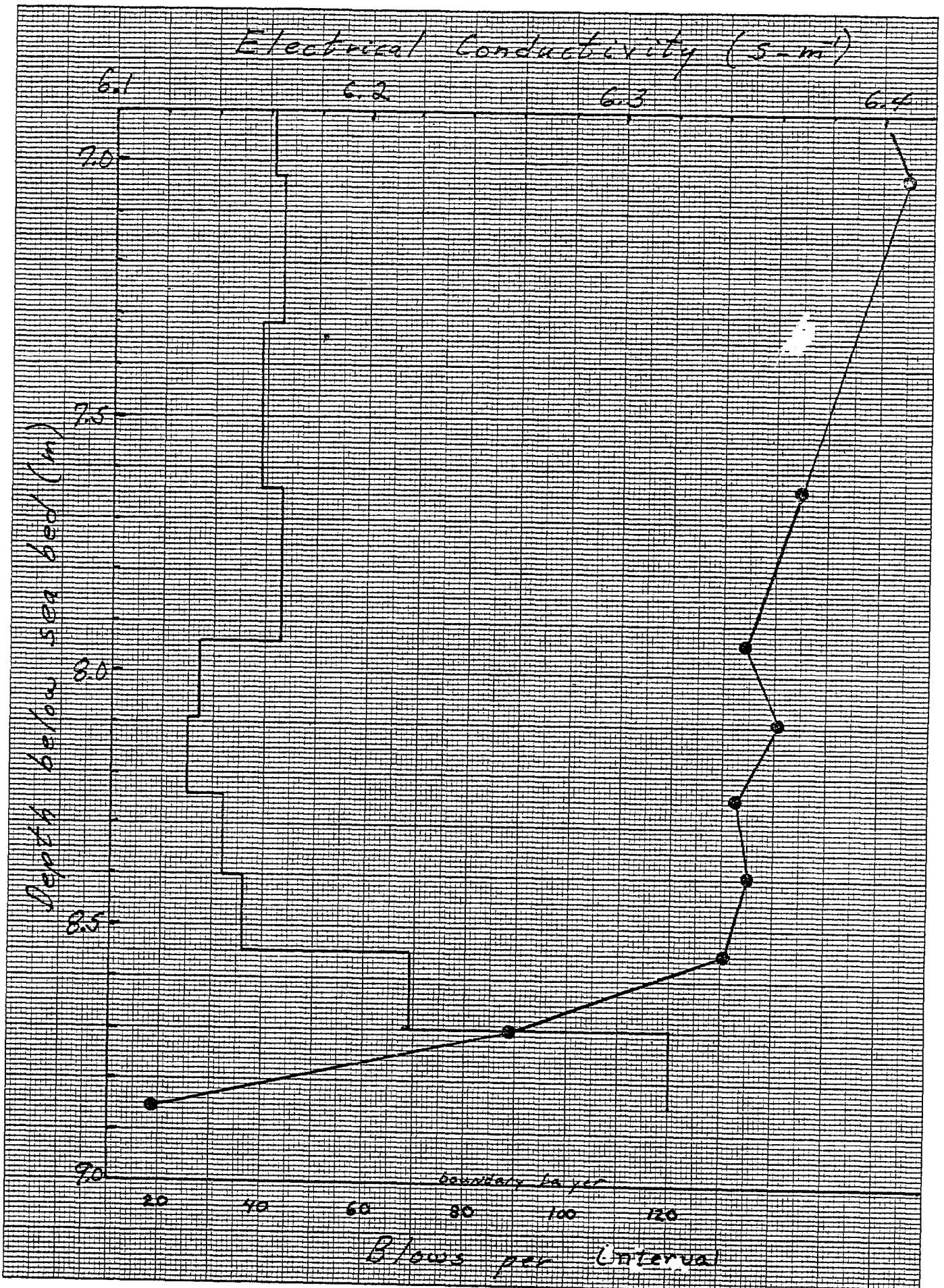


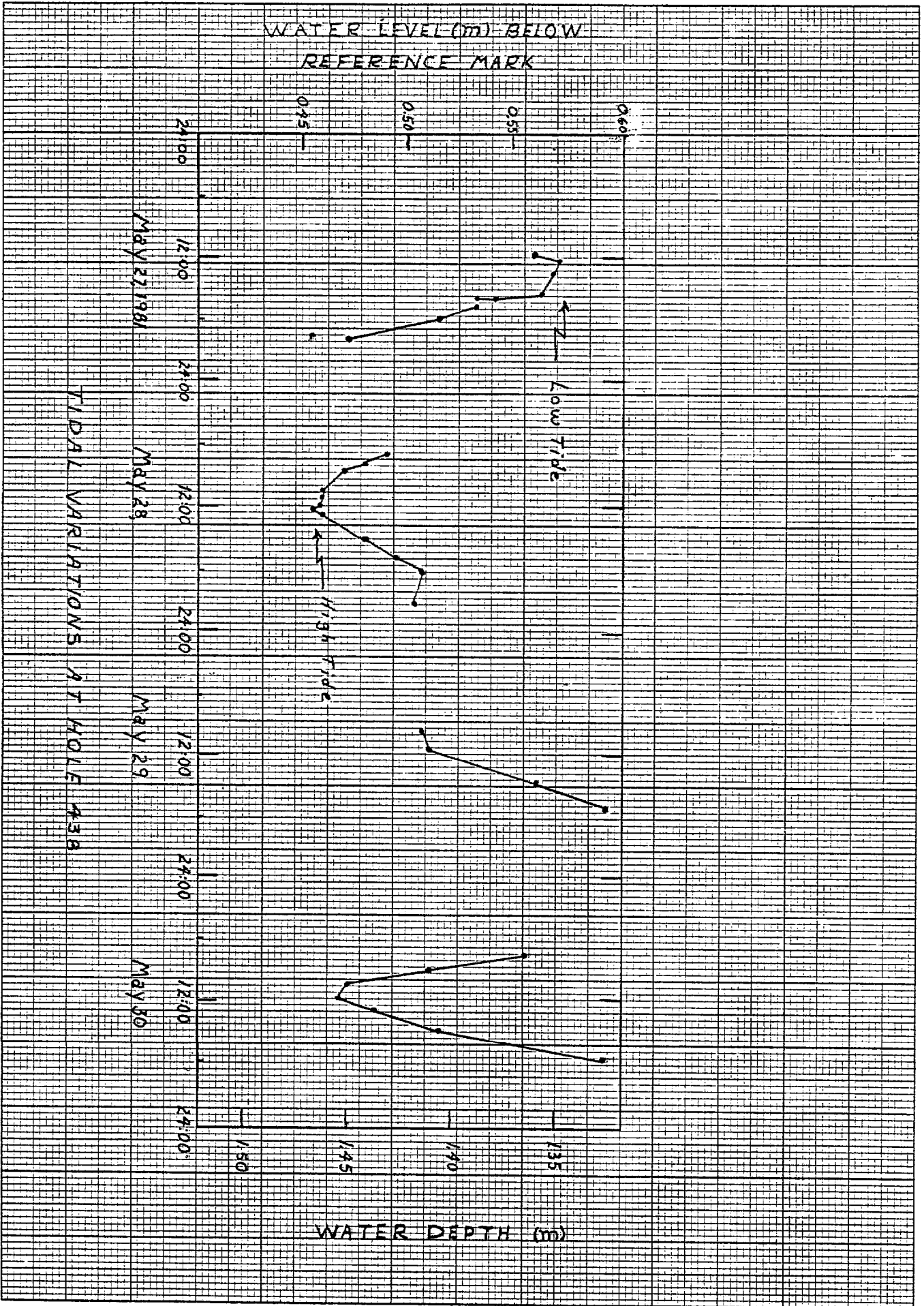
14
70 8.03.9

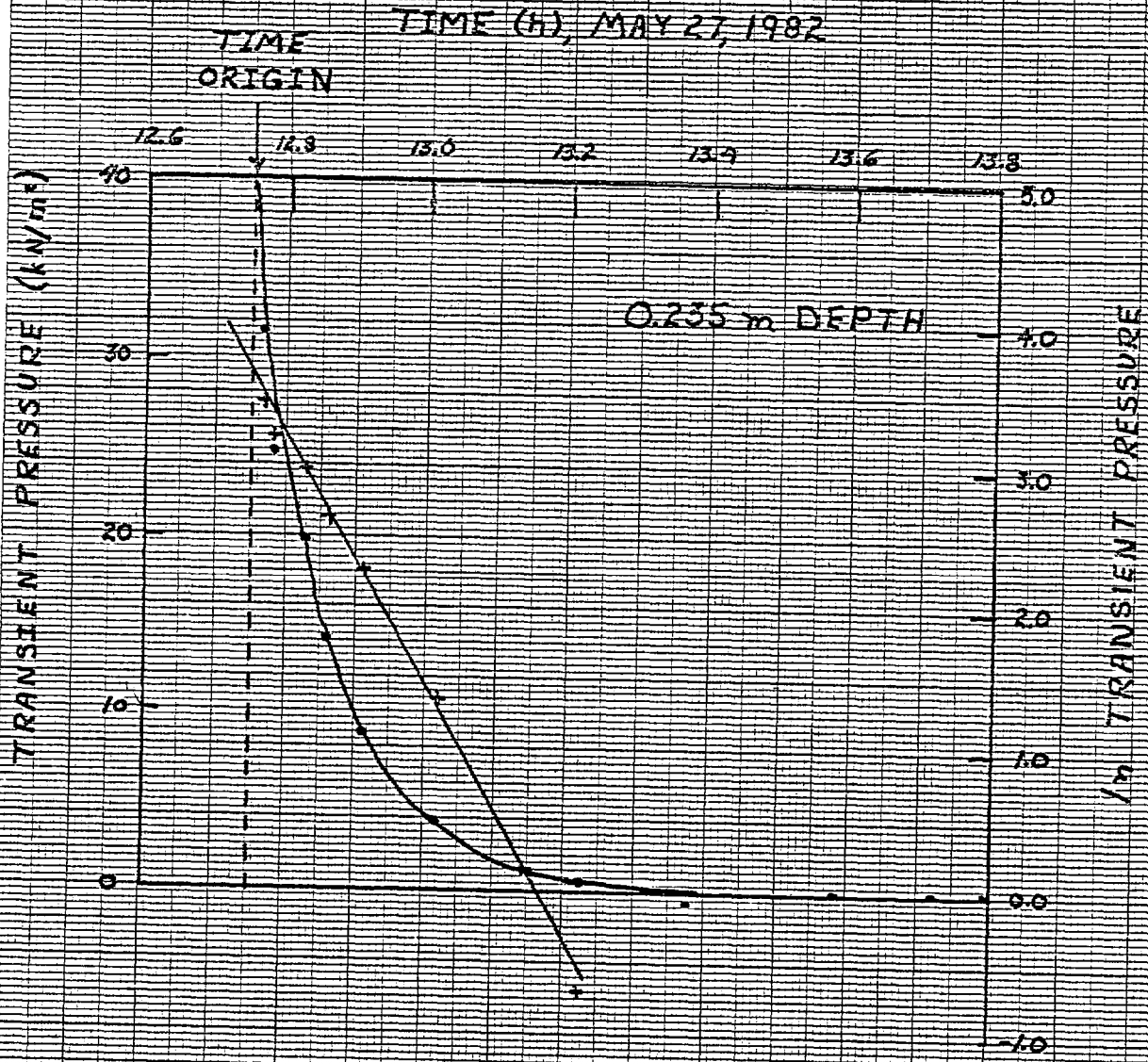


72880729 (5)



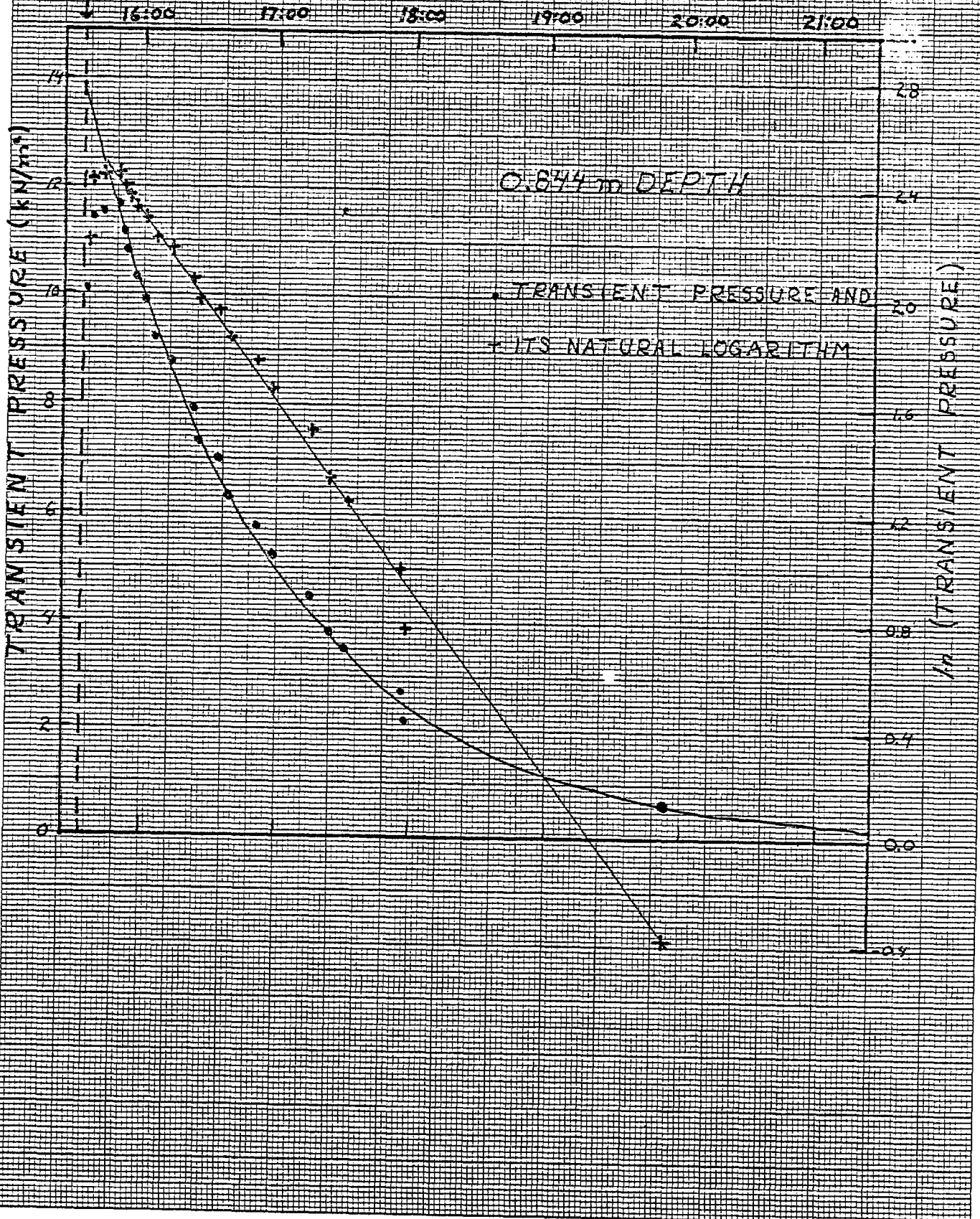




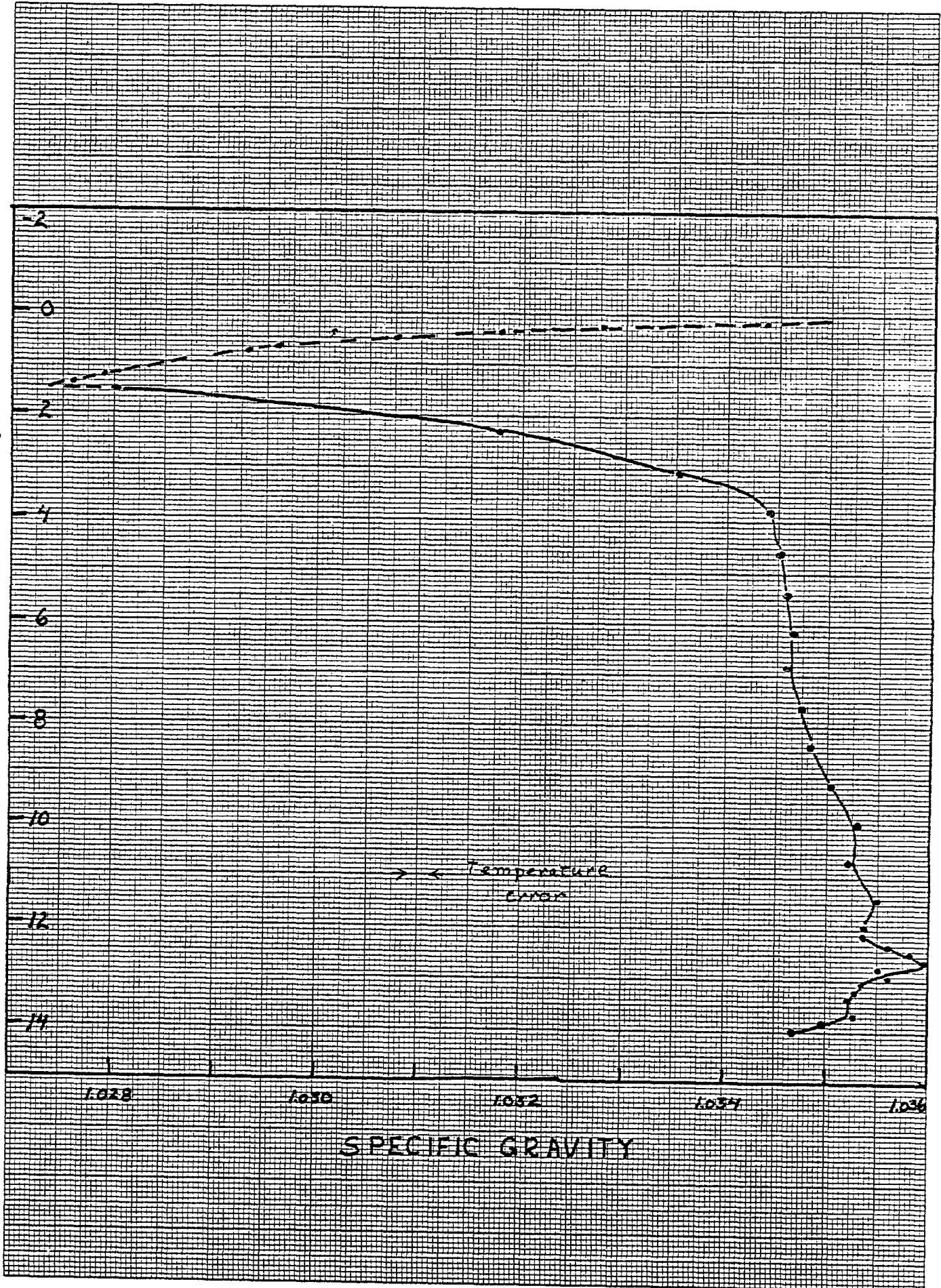


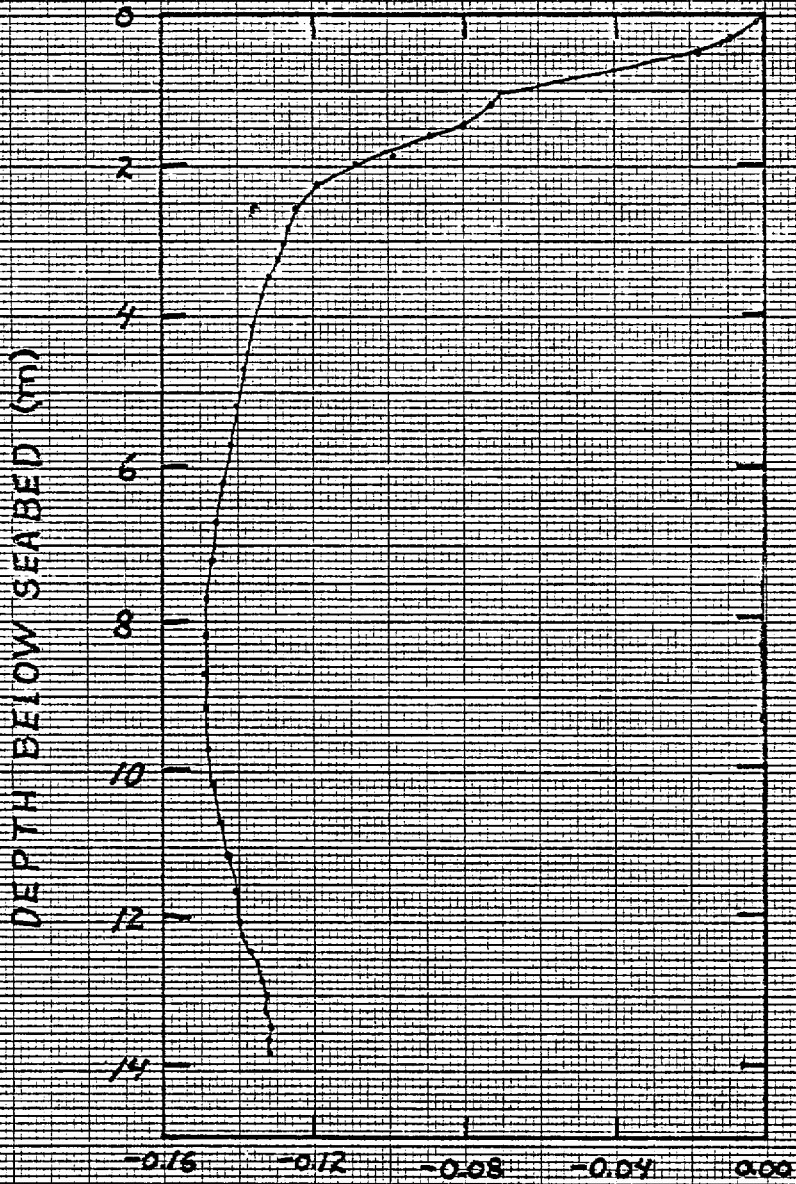
TIME
ORIGIN

TIME (h) MAY 27, 1981



DEPTH BELOW SEABED (m)





HYDROSTATIC PRESSURE RELATIVE
TO CASE WITH CONSTANT SPECIFIC
GRAVITY 1.0350. (kN/m²)

DEPTH BELOW SEABED (m)

PRESSURE MINUS HYDROSTATIC PRESSURE (kN/m²)

3 -2 -1 0 1 2 3 4 5 6

HOLE 440-1981

← Instrumental Sensitivity

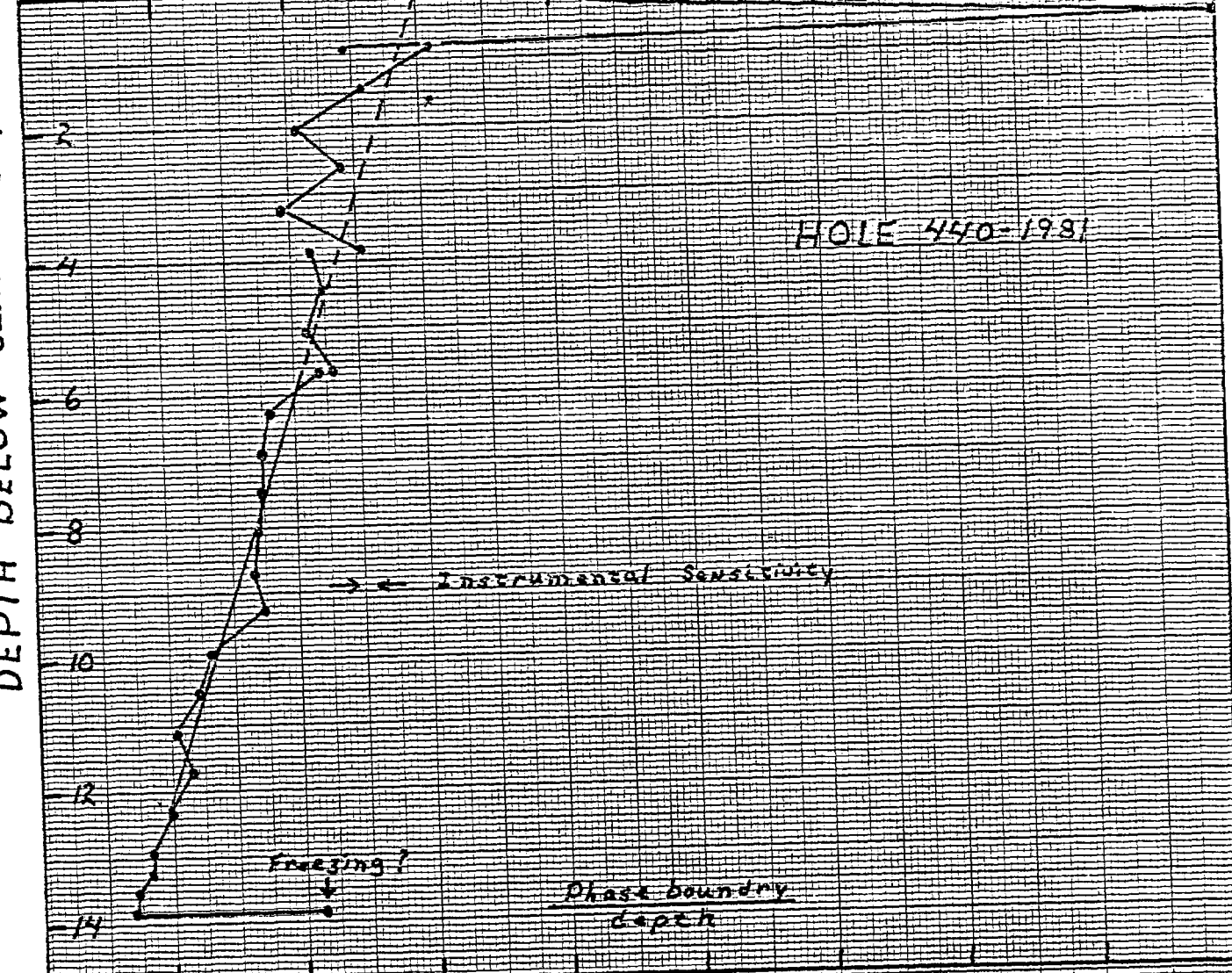
Freezing?

Phase boundary depth

-14

-0.2 -0.1 0 0.1 0.2 0.3 0.4 0.5

PRESSURE MINUS HYDROSTATIC PRESSURE (HEAD, m)



Blows per 0.3 (m)

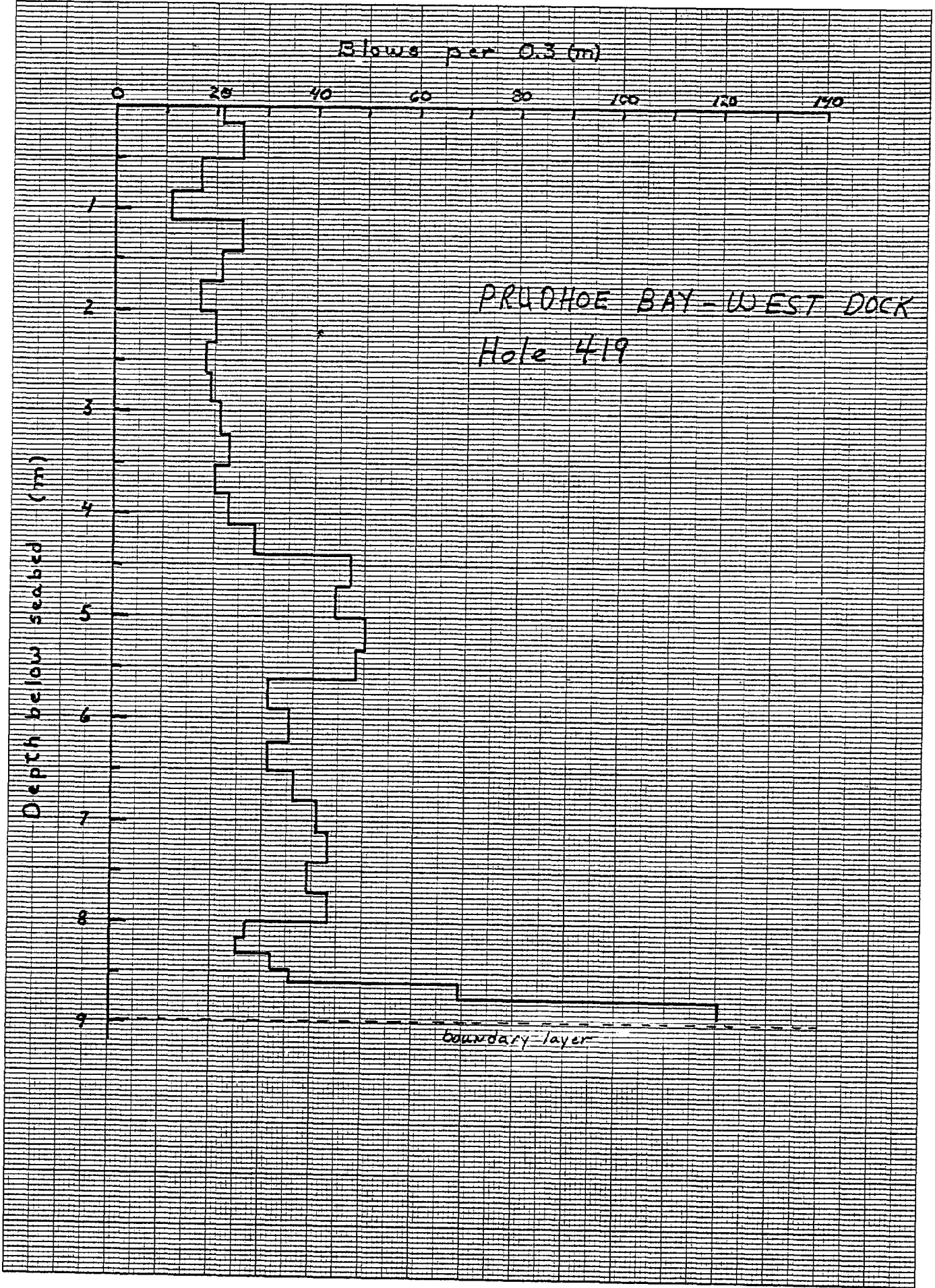
0 25 40 60 80 100 120 140

Depth below seabed (m)

1
2
3
4
5
6
7
8
9

PRUDHOE BAY - WEST DOCK
Hole 419

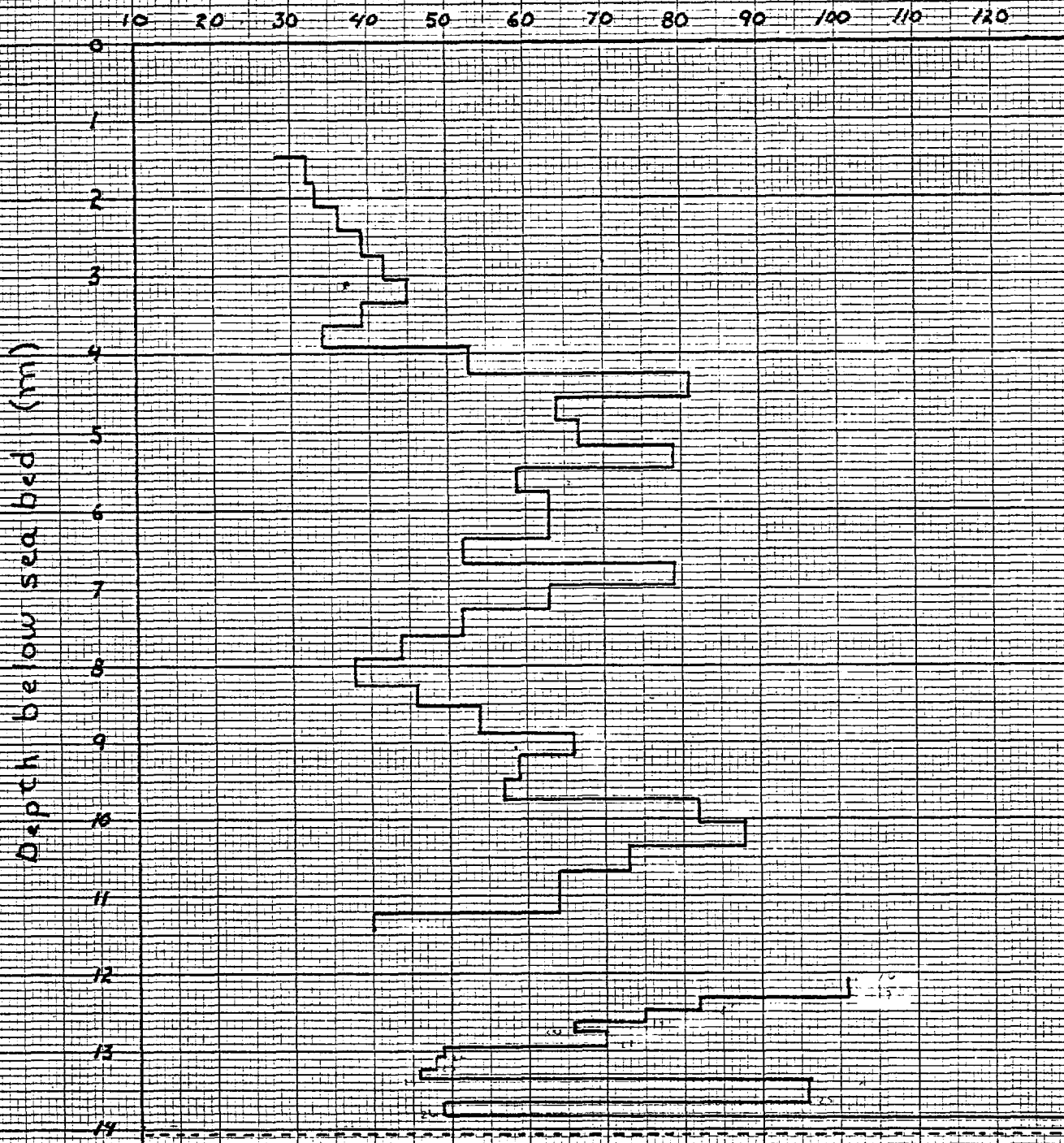
boundary layer



*D 1311

KEUFFEL & ESSER CO. MADE IN U.S.A.

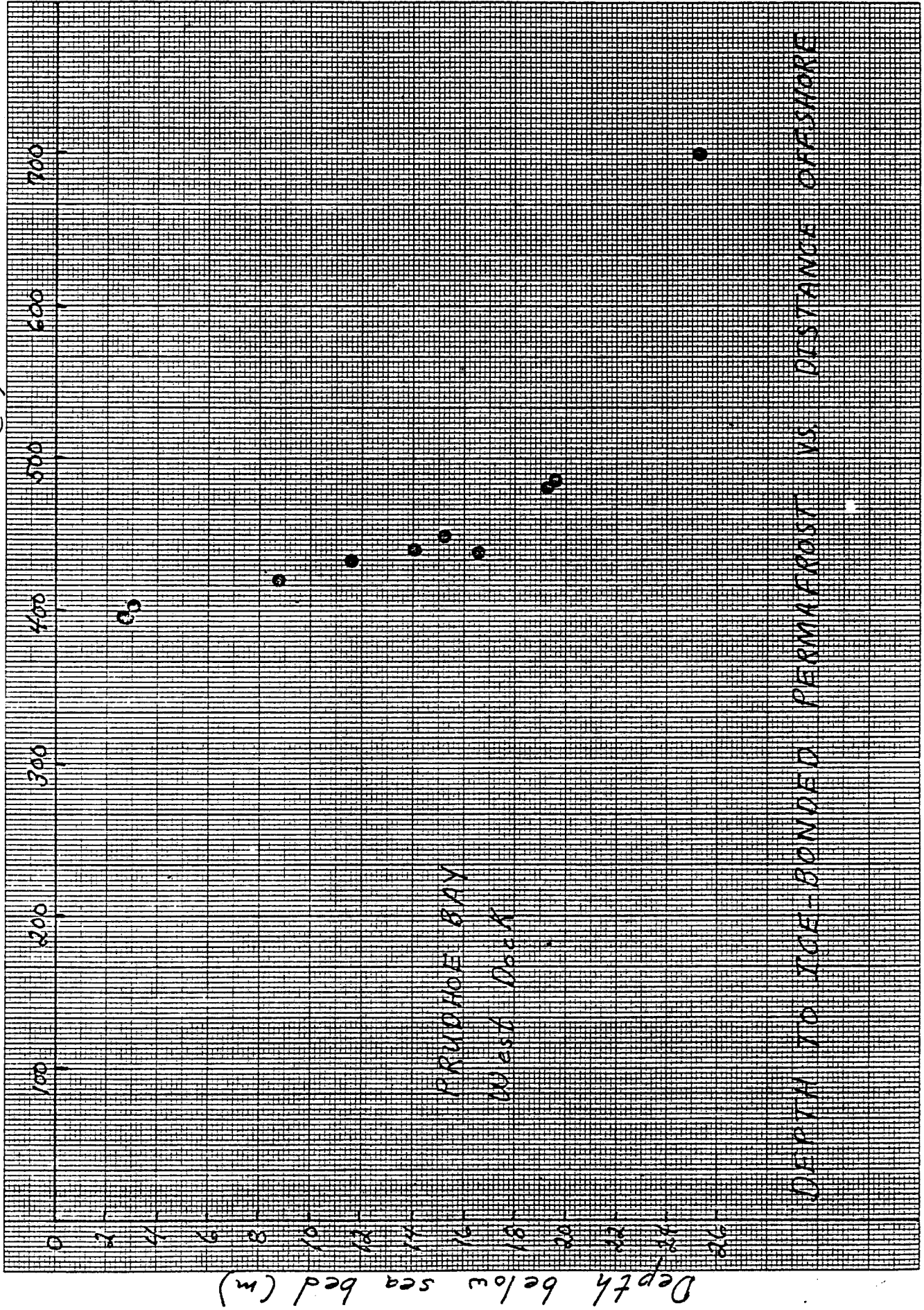
Blows per 0.3 m



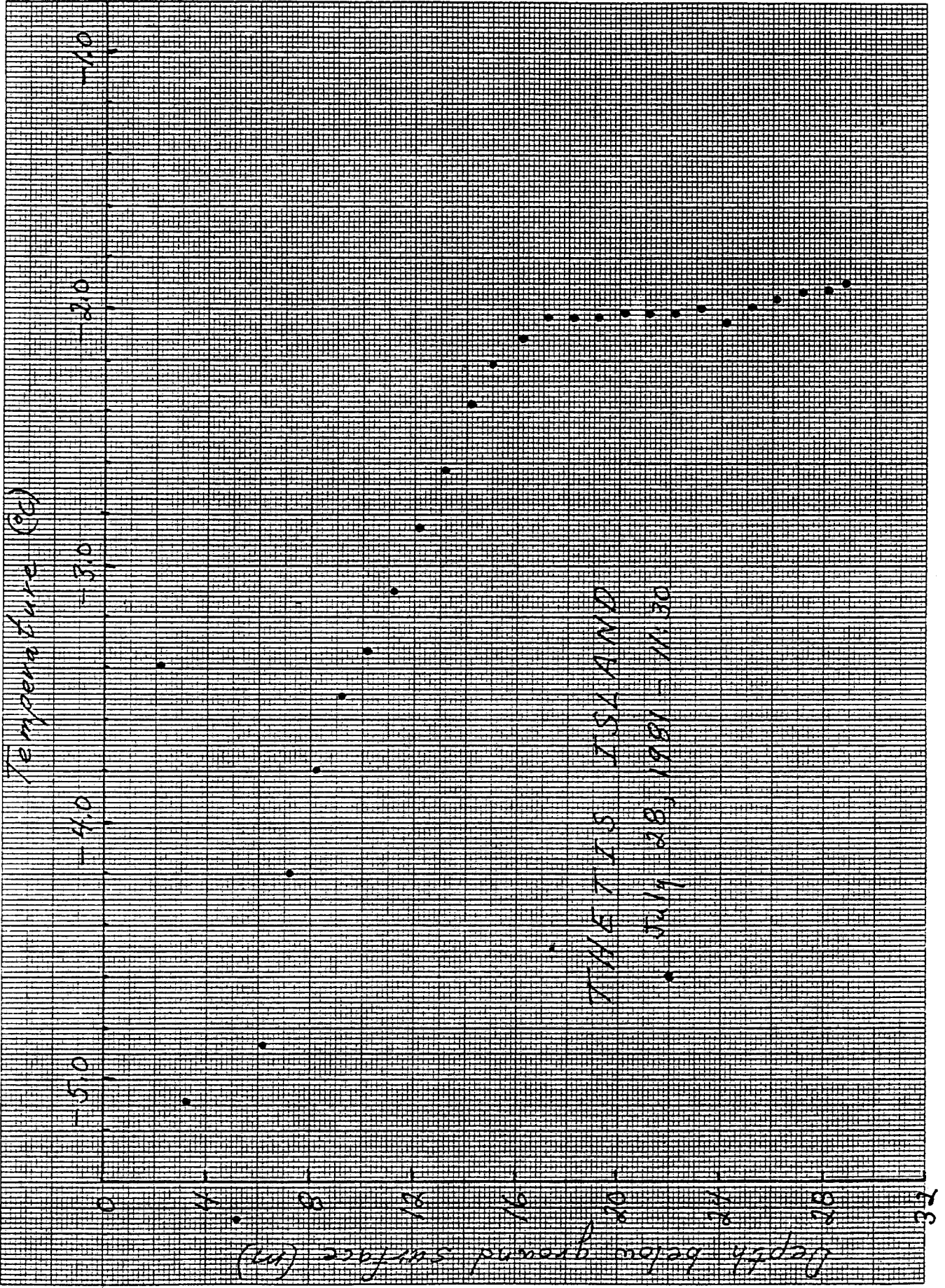
PRUDHOE BAY - WEST DOCK

Hole 439

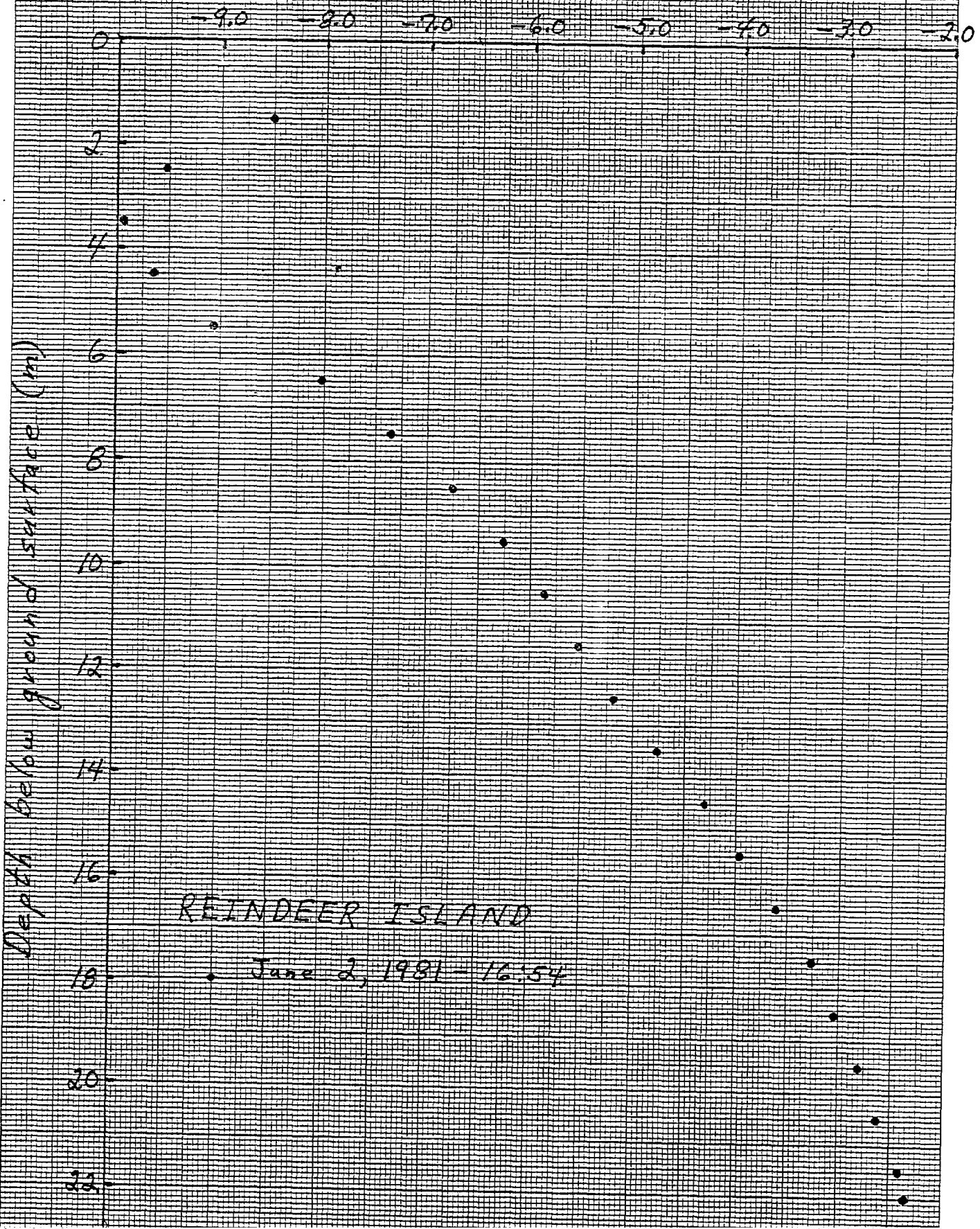
Distance offshore (m)

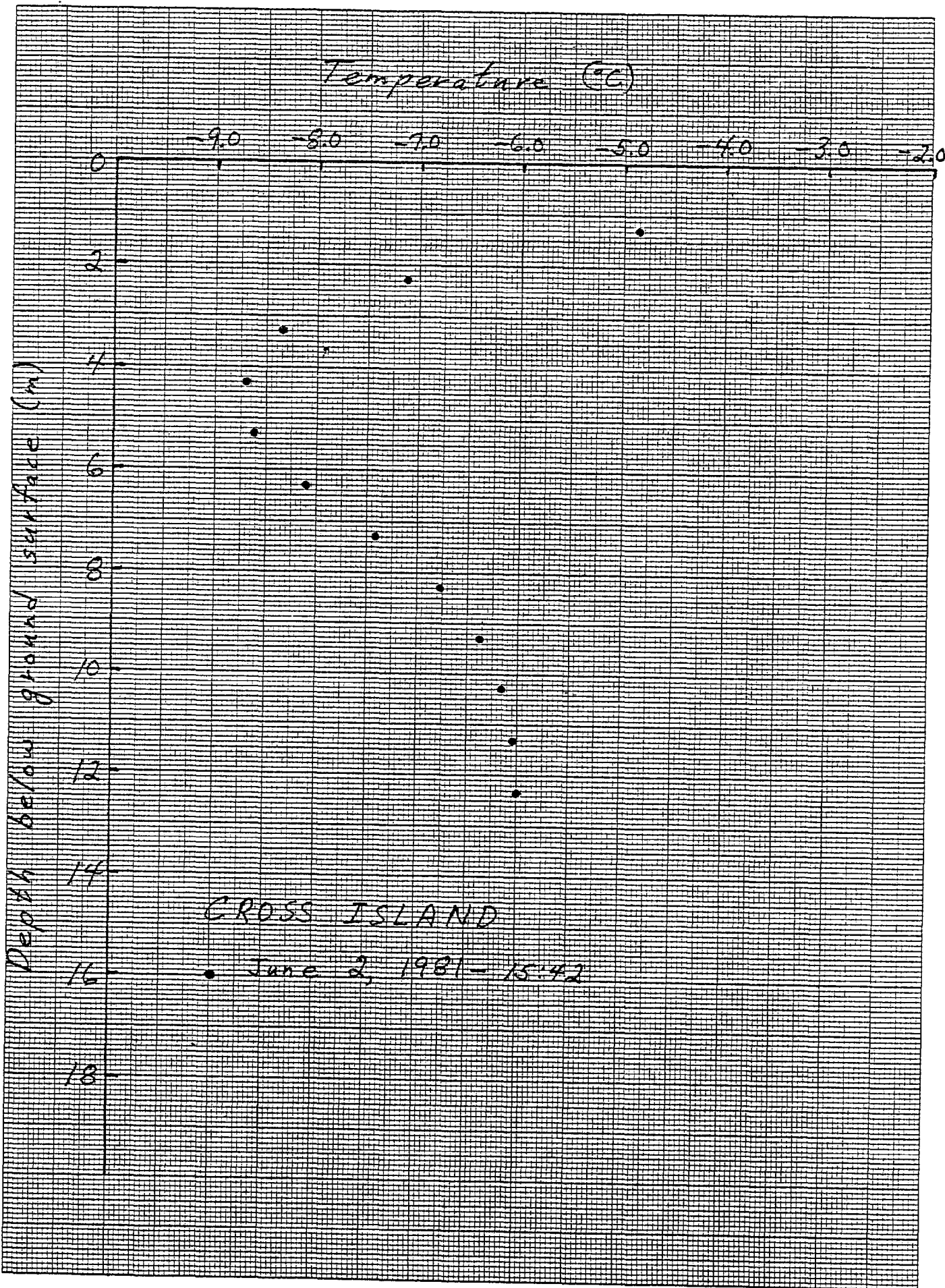


DEPTH TO ICE-BONDED PERMAFROST VS. DISTANCE OFFSHORE



Temperature (°C)





TABLES

- Table 1. Drilling data for holes drilled during the 1981 field season.
- Table 2.** Electrical **conductivities of the** 1981 interstitial water samples from holes 419 and 439 measured **in the** laboratory at 25°C.
- Table 3. Pressure data **from** hole 438.
- Table 4.** Transient pressure behavior.

TABLE 1

Area and Hole Designation	Location	Water Depth (m)	Sea Ice Thickness (m)	Drilling Method	Date of Drilling	Total Depth Below Sea Bed (m)	Date of Temp. Logging
<u>Cape Lisburne</u>							
Hole 1	≈ 25 miles on a heading of 075° magnetic	6.10	1.50	drive	March 27, 1981	No penetration, rock near sea bed	
Hole 2	048° magnetic from Cape Lisburne radome at ≈ 32 miles	17.16	1.51	jet	March 28, 1981	"	
Hole 3	065° magnetic from Cape Lisburne radome at ≈ 37 miles	17.16	1.51	jet	March 28, 1981	"	
Hole 4	357° magnetic from Cape Lisburne radome at ≈ 22 miles	30.48	0.40	jet	March 29, 1981	"	
Hole 5	005° magnetic from Cape Lisburne radome at ≈ 10 miles	21.03	0.72	jet	March 29, 1981	"	
Hole 6	050° magnetic from Cape Lisburne radome at ≈ 55 miles	14.42	0.76	jet	March 30, 1981	"	
Ogotoruk Creek	Hole to Crowbill Pt. , N 303° E; Hole to highest peak of Crowbill Pt. , N313°30'E	6.40	0.81	Not attempted, bottom found to be hard by hand probing	March 31, 1981	No penetration, rock near sea bed	

Area and Hole Designation	Location	Water Depth (m)	Sea Ice Thickness (m)	Drilling Method	Date of Drilling	Total Depth Below Sea Bed (m)	Date of Temp. Logging
Esook A	70°52.24'N 152°25.34'	2.72	1.98	rotary-jet	May 1, 1981	17.59	May 5, 12, 29
Esook B	70°52.48'N 152°21.1'	5.45	1.68	rotary-jet	May 7, 1981	19.27	May 12, 29
Esook C	70°55.35'N 152°21.1'	10.50	1.79	rotary-jet	May 7, 1981	42.77	Pipe broken at sea bed
Thetis A	330° magnetic from Thetis Island hole at 23 naut. miles	25.92	2.82	jetted	April 30, 1981	3.96	Not logged hole lost during casing process
Thetis B	70°39.2'N 150°08.9'W N148.5°E hole to Oliktok radome	14.78	1.81	jetted	April 30, 1981	16.65	May 29
Atigaru Pt.	70°36.4'N 151°30.5'W	6.83	1.86	rotary-jet	May 1, 1981	17.17	May 5, 12, 20, 28
Hole 398	On a line bear- ing N31°E from NPBS #1 well. 398 m offshore.		1.27	driven	May 27, 1981	2.74	June 1, 2
Hole 418	Same, but 418 m offshore		1.51	driven	May 27, 1981	8.81 m	June 1, 2
Hole 419	Same, but 419 m offshore		1.63	driven	May 31, 1981	8.95 m	salinity samples

Area and Hole Designation	Location	Water Depth (m)	Sea Ice Thickness (m)	Drilling Method	Date of Drilling	Total Depth Below Sea Bed (m)	Date of Temp. Logging
Hole 433	Same, but 433m offshore		1.58	driven	May 28, 1981	10.81 m	May 30, June 2
Hole 439	same, but 439 m offshore		1.54-1.67	driven	May 30, 1981	14.09	May 30, June salinity samples
Hole 448	same, but 448 m offshore		1.61	driven	May 28, 1981	15.30	

TABLE 2

Electrical conductivity of 25°C of pore water from hole 419
May 31 - June 1, 1981

Sample Number	Depth Below Sea Bed (m)	Electrical Conductivity (S-m ⁻¹)
	?	
419-1-1981	2.301	5.797
2	3.063	6.018
3	3.825	6.193
4	4.587	6.348
5	5.349	6.383
6	6.416	6.351
7	7.025	6.410
8	7.635	6.369
9	7.940	6.348
10	8.093	6.361
11	8.245	6.345
12	8.398	6.350
13	8.550	6.341
14	8.702	6.257
15	8.855	6.117
16	8.855	(5.532 sample removed after probe pulled)

Note: Ice thickness = 1.63 m. Slush layers made ice-sea bed interface uncertain. Ice thickness could be as little as 1.48 m, in which case the given depths below sea bed would be increased by 0.15 m.

Length of sampler = 0.1 m

TABLE 2

Electrical conductivity at 25°C of pore water from hole 439,
May 28 - May 30, 1981

Sample Number	Depth Below Sea Bed (m)	Electrical Conductivity ($S\cdot m^{-1}$)	Sample Function
	F		
439-1-1981	1.497	5.275	-1.909 T4
2	2.259	5.898	-2.179
3	3.021	6.186	-2.308
4	3.783	6.326	-2.371
5	4.545	6.344	-2.379
6	5.307	6.355	
7	6.069	6.367	
8	6.831	6.355	
9	7*593	6.384	
10	8.355	6.394	
11	9.117	6.429	
12	9.879	6.473	
13	10.641	6.456	
14	11.403	6.504	
15	11.936	6.481	
16	12.165	6.479	
17	12.317	6.515	
18	12.470	6.551	
19	12.622	6.576	
20	12.775	6.504	
21	12.927	6.518	
22	13.080	6.475	
23	13.232	6.467	
24	13.385	6.456	
25	13.689	6.463	
26A	13.841	6.419	
26B	13.841	6.415	
27	13.993	6.206	

Note: Ice thickness \approx 1.67 m. Slush layers made ice-sea bed interface uncertain. Ice thickness could be as little as 1.54 m, in which case the given depths below sea bed would be increased by 0.13 m.

Length of sampler = 0.1 m

TABLE 3 PRESSURE DATA

Date/time (1981) -	Depth below sea bed	Depth below water surface	Pressure (P)	$\rho_r g h$	$-\rho_r g h$	$\int \rho g dh$ $-\rho_r g h$	p $-\int \rho g dh$
	(m)	(in)	(kN/m ²)	(kN/m ²)	(kN/m ²)	(kN/m ²)	(kN/m ²)
May 27							
11.43	-0.070	1.289	12.80	13.11	- 0.31	0.00	- 0.31
later	-0.070	1.278	13.15	13.00	0.15	0.00	0.15
13.43	0.235	1.585	17.69	16.12	1.57	- 0.01	1.58
15.29	0.540	1.892	25.21	19.24	5.97	- 0.02	5.99
20.02	0.844	2.292	23.94*	23.31	- 0.63	- 0.04	- 0.59
May 28							
08.40	0.844	2.294	23.35	23.33	0.02	- 0.04	0.06
09.33	1.149		**				
12.26	1.454	2.918	29.14	29.68	- 0.54	- 0.07	- 0.47
13.57	2.064	3.514	34.65	35.74	- 1.09	- 0.11	- 0.98
15.21	2.673	4.113	41.07	41.83	- 0.76	- 0.13	- 0.63
15.34	2.978		***				
17.08	3.283	4.708	46.65	47.88	- 1.23	- 0.13	- 1.10
21.10	3.892	5.309	53.34	53.99	- 0.65	- 0.14	- 0.51
May 29							
07.04	3.892	5.312	52.99	54.02	- 1.03	- 0.14	- 0.89
09.20	4.502	5.915	59.20	60.15	- 0.95	- 0.14	- 0.81
11.25	5.112	6.522	65.26	66.33	- 1.07	- 0.14	- 0.93
17.10	5.721	7.046	70.78	71.66	- 0.88	- 0.14	- 0.74
May 30							
07.28	5.721	7.084	71.05	72.04	- 0.99	- 0.14	- 0.85
08.49	6.331	7.731	77.26	78.62	- 1.36	- 0.14	- 1.22
09.08	6.940	8.349	83.46	84.91	- 1.45	- 0.15	- 1.30
09.42	7.550	8.980	89.88	91.33	- 1.45	- 0.15	- 1.30
10.04	8.160	9.600	96.15	97.63	- 1.48	- 0.15	- 1*33
10.17	8.772	10.220	102.42	103.94	- 1.52	- 0.15	- 1.37
11.38	9.379	10.831	108.70	110.15	- 1.45	- 0.15	- 1.30
12.16	9.988	11.433	114.42	116.27	- 1.85	- 0.15	- 1.70
12.51	10.604	12.039	120.48	122.44	- 1.96	- 0.15	- 1.81
13.00	11.208	12.638	126.41	128.53	- 2.12	- 0.14	- 1.98
14.00	11.817	13.232	132.55	134.57	- 2.02	- 0.14	- 1.88
14.25	12.427	13.837	138.55	140.72	- 2.17	- 0.14	- 2.03
14.50	13.036	14.441	144.55	146.86	- 2.31	- 0.13	- 2.18
15.12	13.341	14.741	147.58	149.91	- 2.33	- 0.13	- 2.20
15.39	13.646	15.034	150.47	152.89	- 2.42	- 0.13	- 2.29
16.06	13.946	15.316	153.30	155.76	- 2.46	- 0.13	- 2.33
16.40	13.946	15.296	154.54	155.56	- 1.02	- 0.13	- 0.89

* Not quite equilibrated

** Pressure still increasing after 31 min.

*** Pressure still decreasing after 8 min.

TABLE 4 TRANSIENT PRESSURE BEHAVIOUR

Depth Below Sea Bed	Transient Pressure Amplitude (p_t)	Time Constant	Comments
0.235 m	38 kN/m ²	6.7 min.	
0.540	93	13.2	
0.844	14.0	85	Initial rapid increase observed.
1.149			Observations too short to determine transient, but initial increase observed.
1.454	(≈ 5)	(≈ 42)	Transient may be more complicated than exponential.
2.064			Transient rapid, just observable qualitatively.
2.673		≈ 0	Transient very rapid and/or small; not observed.
2.978	not measured		Transient observed.
3.283		≈ 0	Transient very rapid and/or small; not observed at this and all greater depths except at phase boundary.

APPENDIX A

Tabulation of Temperature Data
for the 1981 Field Season

E SOOK A
 HOLE A
 810505
 12:02:00

81-5 CABLE
 OLD L&N BRIDGE

TIME	DEPTH (M)	R (OHMS)	T (C)
12.85	0.88	13089.0	-1.731
12.80	1.88	13097.0	-1.745
12.77	2.88	13122.0	-1.767
12.72	3.88	13142.0	-1.821
12.67	4.88	13157.0	-1.847
12.62	5.88	13169.0	-1.867
12.57	6.88	13183.0	-1.891
12.52	7.88	13187.0	-1.897
12.47	8.88	13196.0	-1.913
12.40	9.88	13196.0	-1.913
12.33	10.88	13201.0	-1.921
12.28	11.88	13198.0	-1.916
12.22	12.88	13220.0	-1.953
12.17	13.88	13203.0	-1.925

E SONS A
HOLE A
810512
11:50:00

81-1 CABLE
OLD L&N-DVM BRIDGE

TIME	DEPTH (M)	R (OHMS)	T (C)
12.77	0.88	14526.0	-1.953
12.72	1.88	14508.0	-1.926
12.63	2.88	14485.0	-1.892
12.58	3.88	14517.0	-1.939
12.52	4.88	14653.0	-2.138
12.47	5.88	14784.0	-2.327
12.43	6.88	14927.0	-2.531
12.37	7.88	15055.0	-2.712
12.32	8.88	15166.0	-2.867
12.25	9.88	15279.0	-3.024
12.18	10.88	15413.0	-3.209
12.13	11.88	15513.0	-3.345
12.08	12.88	15663.0	-3.548
12.02	13.88	15763.0	-3.682

F 50JKH
HOLE A
810529
20:46:00

81-5 CABLE
OLD L&N BRIDGE

TIME	DEPTH (M)	R (OHMS)	T (C)
21.72	0.88	13138.0	-1.814
21.68	1.88	13138.0	-1.814
21.65	2.88	13149.0	-1.833
21.60	3.88	13199.0	-1.918
21.57	4.88	13318.0	-2.118
21.53	5.88	13438.0	-2.318
21.50	6.88	13548.0	-2.499
21.47	7.88	13665.0	-2.690
21.42	8.88	13772.0	-2.863
21.38	9.88	13874.0	-3.026
21.33	10.88	13977.0	-3.190
21.27	11.88	14081.0	-3.354
21.20	12.88	14172.0	-3.496
21.17	13.88	14272.0	-3.651
21.13	14.88	14370.0	-3.801
21.10	15.88	14452.0	-3.927
21.05	16.88	14523.0	-4.034

E SOOK A
HOLE A
810530
00101100

81-5 CABLE
OLD L&N BRIDGE

TIME	DEPTH (M)	R (OHMS)	T (C)
0.65	0.88	12683.0	-1.025
0.62	1.88	12654.0	-0.973
0.58	2.88	12268.0	-0.275
0.53	3.88	12966.0	-1.520
0.50	4.88	13042.0	-1.650
0.47	5.88	13063.0	-1.686
0.43	6.88	13138.0	-1.814
0.40	7.88	13222.0	-1.957
0.37	8.88	13313.0	-2.110
0.33	9.88	13428.0	-2.301
0.30	10.88	13512.0	-2.440
0.27	11.88	13599.0	-2.582
0.22	12.88	13683.0	-2.719
0.18	13.88	13813.0	-2.929
0.15	14.88	13837.0	-2.967
0.12	15.88	13959.0	-3.161
0.07	16.88	14009.0	-3.240

E SOOK B
HOLE B
810512
10:45:00

81-1 CABLE
OLD L&N BRIDGE

TIME	DEPTH (M)	R (OHMS)	T (C)
11.65	0.21	14399.0	-1.766
11.60	1.21	14366.0	-1.717
11.53	2.21	14349.0	-1.691
11.47	3.21	14437.0	-1.822
11.40	4.21	14448.0	-1.838
11.33	5.21	14469.0	-1.869
11.30	6.21	14531.0	-1.960
11.23	7.21	14563.0	-2.007
11.18	8.21	14634.0	-2.110
11.13	9.21	14689.0	-2.190
11.07	10.21	14752.0	-2.281
11.02	11.21	14732.0	-2.252
10.97	12.21	14778.0	-2.318
10.93	13.21	14867.0	-2.417
10.87	14.21	14928.0	-2.532

E SOOK B
 HOLE B
 810529
 16:32:00

81-1
 • OLD L&N CABLE
 BRIDGE

TIME	DEPTH (M)	R (OHMS)	T (C)
17.37	0.21	14414.0	-1.788
17.33	1.21	14395.0	-1.760
17.30	2.21	14384.0	-1.743
17.27	3.21	14380.0	-1.737
17.23	4.21	14376.0	-1.731
17.15	5.21	14389.0	-1.751
17.10	6.21	14442.0	-1.829
17.07	7. 21	14505.0	-1.922
17.02	8.21	14579.0	-2.030
16.98	9.21	14642.0	-2.122
16.93	10.21	1470 3.0	-2.210
16.90	11.21	14762.0	-2.295
16.85	12.21	14823.0	-2.383
16.82	13.21	14880.0	-2. 464
16.78	14.21	14929.0	-2.534
16.72	15.21	14977.0	-2.602
16.68	16.21	15013.0	-2.653
16. 65	17.21	15063.0	-2.723

E SOOK B
 HOLE B HEATED
 810529
 19:50:00

810-1 CABLE
 OLD L&N BRIDGE

TIME	DEPTH (M)	K (UNAS)	T (C)
20.40	0.21	14350.0	-1.693
20.37	1.21	13699.0	-0.700
20.33	2.21	13694.0	-0.692
20.30	3.21	13608.0	-0.557
20.27	4.21	13589.0	-0.527
20.23	5.21	13758.0	-0.792
20.20	6.21	14136.0	-1.372
20.17	7.21	14325.0	-1.656
20.15	8.21	14348.0	-1.690
20.12	9.21	14261.0	-1.560
20.10	10.21	1435 3.0	-1.697
20.07	11.21	14363.0	-1.712
20.03	12.21	14390.0	-1.752
20.00	13.21	14424.0	-1.803
19.97	14.21	14476.0	-1.879
19.93	15.21	14553.0	-1.992
19.90	16.21	14558.0	-1.999
19. 88	17.21	14527.0	-1.954

ATIGARU POINT
 HOLE AP-1
 810505
 14:15:00

81-1 CABLE
 OLD L&N BRIDGE

TIME	DEPTH (M)	R (OHMS)	T (C)
15.17	0.43	14392.0	-1.755
15.13	1.43	14292.0	-1.607
15.10	2.43	14217.0	-1.494
15.05	3.43	14159.0	-1.407
15.02	4.43	14124.0	-1.354
14.95	5.43	14110.0	-1.333
14.88	6.43	14100.0	-1.318
14.85	7.43	14099.0	-1.316
14.80	8.43	14104.0	-1.324
14.72	9.43	14109.0	-1.331
14.68	10.43	14118.0	-1.345
14.63	11.43	14131.0	-1.365
14.57	12.43	14144.0	-1.384
14.53	13.43	14148.0	-1.390
14.48	14.43	14125.0	-1.356
14.43	15.43	14077.0	-1.283
14.38	16.43	14057.0	-1.252

* LIST AT0.2
 (50)FILE AT0.2 -- NON-EXISTENT

* LIST AT0.2

1

AT0.2
 HOLE AP-2
 810512
 16:25:00

01-1 CABLE
 OLD L&N BRIDGE

TIME	DEPTH (M)	R (OHMS)	T (C)
17.00	0.43	14437.0	-1.822
37	1.43	14390.0	-1.764
1.2.00	2.43	14314.0	-1.639
17.11	3.43	14235.0	-1.526
	4.43	14120.0	-1.499
	5.43	14157.0	-1.404
	6.43	14117.0	-1.344
17.14	7.43	14082.0	-1.315
	8.43	14090.0	-1.298
17.17	9.43	14092.0	-1.312
	10.43	14120.0	-1.348
17.20	11.43	14110.0	-1.348
	12.43	14177.0	-1.398
17.23	13.43	14177.0	-1.434
	14.43	14102.0	-1.368
17.26	15.43	14101.0	-1.368
16.50	16.43	14155.0	-1.401

* LIST ATIG3

1

ATICARU POINT
HOLE AP-3
810521
09:56:00

	Ø1-1 OLD LAN	CABLE BRIDGE	
TIME	DEPTH (M)	R (OHMS)	T (C)
10.70	0.43	14388.0	-1.749
10.67	1.43	14299.0	-1.617
10.62	2.43	14259.0	-1.557
10.58	3.43	14196.0	-1.463
10.55	4.43	14143.0	-1.383
10.50	5.43	14122.0	-1.351
10.47	6.43	14112.0	-1.336
10.43	7.43	14109.0	-1.331
10.38	8.43	14110.0	-1.333
10.35	9.43	14110.0	-1.333
10.28	10.43	14111.0	-1.334
10.23	11.43	14122.0	-1.351
10.20	12.43	14133.0	-1.368
10.15	13.43	14142.0	-1.381
10.10	14.43	14147.0	-1.389
10.07	15.43	14151.0	-1.395
10.03	16.43	14156.0	-1.402

ATIGARU POINT
HOLE AP-4
810528
15:39:00

CABLE
BRIDGE

TIME	DEPTH (M)	R (OHMS)	T (C)
16.55	0.43	14390.0	-1.752
16.50	1.43	14364.0	-1.714
16.47	2.43	14311.0	-1.635
16.43	3.43	14265.0	-1.566
16.38	4.43	14141.0	-1.380
16.35	5.43	14116.0	-1.342
16.27	6.43	14109.0	-1.331
16.22	7.43	14105.0	-1.325
16.13	8.43	14108.0	-1.330
16.10	9.43	14109.0	-1.331
16.07	10.43	14118.0	-1.345
16.02	11.43	14125.0	-1.356
15.98	12.43	14133.0	-1.368
15.93	13.43	14133.0	-1.368
15.87	14.43	14134.0	-1.369
15.82	15.43	14140.0	-1.378
15.77	16.43	14140.0	-1.378

ATIGARD POINT
HOLE AP-5
810528
19100100

81-1 CARLE
OLD CAN BRIDGE

TIME	DEPTH (ft)	W. (lb)	W. (lb)
19.65	0.43	14302.0	-1.621
19.62	1.43	14128.0	1.360
19.58	2.43	14045.0	-1.534
19.55	3.43	14027.0	-1.207
19.52	4.43	13704.0	-0.708
19.47	5.43	13697.0	-0.697
19.43	6.43	13681.0	-0.672
19.38	7.43	13728.0	-0.739
19.35	8.43	13674.0	-0.641
19.32	9.43	13639.0	-0.599
19.27	10.43	13488.0	-0.360
19.22	11.43	13478.0	-0.376
19.18	12.43	14104.0	-1.104
19.15	13.43	14149.0	-1.305
19.12	14.43	14165.0	-1.356
19.09	15.43	14152.0	-1.356
19.06	16.43	14188.0	-1.405
19.03	17.43	14172.0	-1.427

PRUDHOE BAY
HOLE 398
810601
18:30:00

81-1
OLD L&N
CABLE
BRIDGE

TIME	DEPTH (M)	R (OHMS)	T (C)
18.62	0.84	14853.0	-2.426
18.68	1.84	14604.0	-2.066
18.77	2.31	14615.0	-2.082

PRUDHOE BAY
HOLE 398
810601
18:51:00

81-5
OLD L&N
CABLE
BRIDGE

TIME	DEPTH (M)	R (OHMS)	T (C)
18.90	0.84	13503.0	-2.425
18.97	1.84	13284.0	-2.061
19.03	2.31	13293.0	-2.076

PRUDHOE BAY
HOLE 398
810602
11:15:00

81-1
OLD L&N
CABLE
BRIDGE

TIME	DEPTH (M)	R (OHMS)	T (C)
11.33	0.84	14874.0	-2.456
11.38	1.84	14620.0	-2.090
11.43	2.31	14623.0	-2.094

PRUINHOE BAY
 HOLE 419
 810601
 14:01:00

81-5 CABLE
 01018" BRIDGE

TIME	DEPTH (M)	R (DNMS)	T (C)
16.70	1.77	14523.0	-1.948
16.60	2.11	14552.0	-1.991
16.50	3.27	14583.0	-2.036
16.40	4.77	14629.0	-2.103
16.33	5.77	14679.0	-2.175
16.27	6.77	14728.0	-2.246
16.18	7.77	14765.0	-2.299
16.10	8.72	14813.0	-2.368

PRUDHOE BAY
HOLE 418
810601
17:14:00

81-5
OLD L&N

CABLE
BRIDGE

TIME	DEPTH (M)	R (OHMS)	T (C)
17.32	1.77	13210.0	-1.936
17.48	2.77	13239.0	-1.985
17.62	3.77	13269.0	-2.036
17.75	4.77	13307.0	-2.100
17.92	5.77	13350.0	-2.171
18.03	6.77	13389.0	-2.236
18.20	7.77	13429.0	-2.303
18.37	8.72	13468.0	-2.367

* WAIT

FRIDGE BAY
 HOLE 418
 810602
 10:20:00

81-1 CABLE
 OLD LAY BRIDGE

TIME	DEPTH (M)	R (OHMS)	T (C)
10.82	1:27	14524.0	-1.950
10.88	2:17	14550.0	-1.988
10.93	3:77	14586.0	-2.040
10.98	4:37	14630.0	-2.104
11.02	5:77	714685.0	-2.184
11.07	6:27	14722.0	-2.238
11.10	7:77	14772.0	-2.310
11.17	8:72	14822.0	-2.381

FRUDDHOLE BAY
HOLE 433
810531
06142100

81-1 CABLE
OLD LAN BRIDGE

TIME	DEPTH (M)	R (OHMS)	T (C)
6.78	0.53	14730.0	-2.249
6.87	1.53	14497.0	-1.910
6.95	2.53	14472.0	-1.873
7.03	3.53	14470.0	-1.870
7.10	4.53	14434.0	-1.817
7.15	5.53	14511.0	-1.931
7.25	6.53	14547.0	-1.983
7.33	7.53	14592.0	-2.049
7.47	8.53	14645.0	-2.126
7.55	9.53	14701.0	-2.207
7.65	10.53	14764.0	-2.298

PRUDHOE BAY
HOLE 433
810602
11:35:00

81-1
OLD L&M
CABLE
BRIDGE

TIME	DEPTH (M)	R (OHMS)	T (C)
11.65	0.53	14733.0	-2.253
11.68	1.53	14505.0	-1.922
11.75	2.53	14475.0	-1.878
11.82	3.53	14473.0	-1.875
11.85	4.53	14436.0	-1.820
11.90	5.53	14516.0	-1.938
11.95	6.53	14552.0	-1.991
12.00	7.53	14597.0	-2.056
12.07	8.53	14648.0	-2.130
12.12	9.53	14705.0	-2.213
12.15	10.53	14767.0	-2.302

PRUDHOE BAY
 HOLE 438
 810531
 08:17:00

81-1 CABLE
 OLD L&N BRIDGE

TIME	DEPTH (M)	R (OHMS)	T (C)
8.30	0.75	14576.0	-2.026
8.37	1.75	14449.0	-1.839
8.45	2.75	14419.0	-1.795
8.50	3.75	14411.0	-1.783
8.55	4.75	14422.0	-1.800
8.63	5.75	14442.0	-1.829
8.67	6.75	14470.0	-1.870
8.72	7.75	14510.0	-1.929
8.77	8.75	14550.0	-1.988
8.82	9.75	14599.0	-2.059
8.87	10.75	14648.0	-2.130
8.93	11.75	14696.0	-2.200
9.05	12.75	14749.0	-2.277
9.10	13.75	14802.0	-2.353
9.18	13.99	14806.0	-2.358

PRUDHOE BAY
HOLE 438
S10402
09109100

S1-11' CABLE
OLD LAN BRIDGE

TIME	DEPTH (M)	R (OHMS)	T (C)
9.20	0.75	14572.0	-2.020
9.25	1.75	14453.0	-1.845
9.28	2.75	14416.0	-1.791
9.33	3.75	14416.0	-1.791
9.37	4.75	14424.0	-1.803
9.42	5.75	14445.0	-1.834
9.47	6.75	14474.0	-1.876
9.52	7.75	14511.0	-1.931
9.55	8.75	14550.0	-1.988
9.60	9.75	14599.0	-2.059
9.65	10.75	14650.0	-2.133
9.70	11.75	14697.0	-2.201
9.75	12.75	14750.0	-2.278
9.80	13.75	14805.0	-2.357
9.83	13.99	14809.0	-2.363

PRUDHOE BAY
HOLE 448
S10531
09:24:00

S1-1 CABLE
OLD L&N BRIDGE

TIME	DEPTH (M)	R (OHMS)	T (C)
9.42	0.72	14633.0	-2.109
9.48	1.72	14415.0	-1.789
9.53	2.72	14402.0	-1.770
9.58	3.72	14388.0	-1.749
9.62	4.72	14382.0	-1.740
9.68	5.72	14388.0	-1.749
9.78	6.72	14409.0	-1.780
9.85	7.72	14443.0	-1.831
9.93	8.72	14490.0	-1.900
9.98	9.72	14535.0	-1.966
10.03	10.72	14583.0	-2.036
10.07	11.72	14637.0	-2.114
10.13	12.72	14690.0	-2.191
10.18	13.72	14747.0	-2.274
10.25	14.72	14801.0	-2.351
10.32	15.16	14819.0	-2.377

PRUDHOE BAY
 HOLE 448
 810602
 08:05:00

S1-1 CABLE
 OLD L&N BRIDGE

TIME	DEPTH (M)	R (OHMS)	T (C)
8.15	0.72	14639.0	-2.117
8.20	1.72	14422.0	-1.800
8.23	2.72	14409.0	-1.780
8.27	3.72	14398.0	-1.764
8.32	4.72	14387.0	-1.748
8.35	5.72	14396.0	-1.761
8.40	6.72	14414.0	-1.788
8.45	7.72	14449.0	-1.839
8.50	8.72	14497.0	-1.910
8.55	9.72	14543.0	-1.977
8.60	10.72	1458 5.0	-2.039
8.63	11.72	14645.0	-2.126
8.70	12.72	14695.0	-2.199
8.75	13.72	14752.0	-2.281
8.80	14.72	14806.0	-2.358
8.87	15.16	14824.0	-2.384

WEIS1: null file

THETIS ISLAND
HOLE 1
810728
11.30:00

81-5 CABLE
OLD MAN BRIDGE

TIME	DEPTH (M)	R (OHMS)	T (C)
13.32	1.24	12108.0	0.022
13.22	2.24	14102.0	-3.386
13.13	3.24	15238.0	-5.086
13.07	4.24	15807.0	-5.882
13.00	5.24	15562.0	-5.543
12.93	6.24	15083.0	-4.863
12.87	7.24	14632.0	-4.198
12.80	8.24	14365.0	-3.794
12.73	9.24	14180.0	-3.508
12.67	10.24	14068.0	-3.330
12.60	11.24	13918.0	-3.096
12.55	12.24	13765.0	-2.852
12.48	13.24	13622.0	-2.620
12.45	14.24	13469.0	-2.369
12.37	15.24	13375.0	-2.213
12.32	16.24	13315.0	-2.113
12.27	17.24	13265.0	-2.029
12.22	18.24	13265.0	-2.029
12.12	19.24	13264.0	-2.027
12.05	20.24	13255.0	-2.012
12.00	21.24	13252.0	-2.007
11.97	22.24	13253.0	-2.009
11.92	23.24	13244.0	-1.994
11.85	24.24	13279.0	-2.053
11.82	25.24	13240.0	-1.987
11.77	26.24	13232.0	-1.957
11.68	27.24	13208.0	-1.933
11.60	28.24	13204.0	-1.926
11.58	28.94	13188.0	-1.899

Reindeer Island
 HOLE reis 2
 811215
 00:00:00

81-1 CABLE
 old lan BRIDGE

TIME	DEPTH (M)	R (OHMS)	T (C)
17.90	1.48	19893.0	-8.502
17.85	2.48	20923.0	-9.528
17.82	2.48	21346.0	-9.932
17.75	4.48	21063.0	-9.663
17.68	5.48	20450.0	-9.064
17.63	6.48	19427.0	-8.018
17.58	7.48	18807.0	-7.353
17.53	8. 48	18253.0	-6.738
17.48	9.48	17838.0	-6.263
17.42	10.48	17505.0	-5.872
17.38	11.48	1721 8.0	-5.529
17.35	12.48	16738.0	-5.188
17.30	13.48	16604.0	-4.772
17.25	14.48	16266.0	-4. 299
17.20	15.48	15974.0	-3.962
17.17	16.48	15704.0	-3.603
17.13	17.48	15453.0	-3.264
17. 08	18.48	15282.0	-3.029
17.05	19.48	15123.0	-2.807
17.00	20.48	14987.0	-2.616
16.97	21 .48	14848.0	-2.418
16.92	22.02	14804.0	-2.355

CROSS ISLAND
 HOLE 1
 810602
 15:42:00

81-1 CABLE
 OLD LAN BRIDGE

TIME	DEPTH (M)	R (OHMS)	T (C)
16.52	1.32	16663.0	-4.846
16.45	2.32	18602.0	-7.128
16.32	3.32	19735.0	-8.339
16.25	4.32	20088.0	-8.701
16.20	5.32	20002.0	-8.613
16.15	6.32	19513.0	-8.108
16.10	7.32	18862.0	-7.413
16.05	8.32	18286.0	-6.775
16.00	9.32	17938.0	-6.378
15.93	10.32	17746.0	-6.156
15.85	11.32	17648.0	-6.041

APPENDIX B

Sediment in Sea Ice Studies

*

-

Sediment in Sea Ice Studies

T. E. Osterkamp

and

J. P. Gosi nk

Investigations during 1981 included laboratory work on sea ice cores to determine the manner in which sediment inclusions were incorporated into the sea ice structure. The results of this research will be combined with an analysis of mechanisms for the incorporation of sediment into the sea ice and will be published in a book on the Beaufort Sea (Barnes, Reimnitz and Schell, editors).

APPENDIX C

Publications

A Probe Method for Soil Water Sampling and Subsurface Measurements

W. D. HARRISON AND T. E. OSTERKAMP

Geophysical Institute, University of Alaska, Fairbanks, Alaska 99701

A technique employing lightweight driving and sampling equipment to obtain interstitial soil water samples is described. It can also be used for hydraulic conductivity, temperature, and water pressure measurements. The sampler consists of a probe, with a shield, a porous metal filter and a check valve which are connected to the surface by plastic tubing inside standard EW or A drill rod. The water sample is collected with a bailer lowered inside the tubing from the surface. The tubing can then be cleared and sealed without pulling the drill rod and the sampler driven to the next depth. A method of estimating the probe shape factor is given. Some of the difficulties unique to sampling interstitial water in thawed subsea permafrost are discussed.

INTRODUCTION

A portable and inexpensive method of obtaining interstitial soil water samples in inaccessible locations has been developed. The method also permits in situ estimates of hydraulic conductivity and pressure and provides access holes for temperature measurements. It is designed to be used in the saturated zone, and it works best in the permeable, relatively coarse-grained sediments which are the most difficult to sample by a more conventional method that requires soil sampling and subsequent water extraction from the sample. The method requires driving a probe, or well point, and therefore only unconsolidated material can be sampled. The maximum depth from which samples have been recovered is 27 m. Several water sampling methods with some similarities to this one have been reported [Wood, 1973; Hansen and Harris, 1974; Yare, 1975; Pickens et al., 1978]. Most of these are best suited for groundwater monitoring over long periods of time or they require a drill rig. Our method has been used in subsea permafrost research, as discussed in more detail in the last section of this paper. Lewellen [1973], Blouin et al. [1979a,b] and Osterkamp and Harrison [1981] have designed somewhat different probing methods for subsea permafrost investigations.

A sketch of a typical setup is shown in Figure 1. The soil water samples enter the collection system through a porous metal filter in the probe, or well point, on the bottom of a string of drive rod. The rate at which the water enters, as measured with a water level sensor lowered inside the rod from the surface (Figure 2), determines the hydraulic conductivity [Luthin and Kirkham, 1949]. When sufficient water has entered, the level sensor is removed and a bailer is used to bring the water sample to the surface. Then the system is cleared of the remaining water, and a check valve at the bottom is automatically closed by pressurizing the system from the surface with a bicycle tire pump. The probe is then driven to the next sampling depth, the pressure released to admit the next sample, and the cycle repeated. Since it is not necessary to remove ('to pull' in drilling terminology) the probe between samples, the method is very efficient.

Most of our samples have been obtained in silty, sandy gravels which have a hydraulic conductivity in the range from 1 to 10 m per year. In this material a sufficient amount

of sample is usually obtained within a few minutes of pressure release. Samples have also been obtained in fine-grained material having a hydraulic conductivity 2 or 3 orders of magnitude less, but the sampling time for these is of the order of 1 day. In this case, several adjacent probes are driven to allow simultaneous sample collection from different depths and the collection system is evacuated with a small hand pump to increase the effective collection head.

Borehole temperature measurements, if necessary, can be made as soon as sampling is completed. However, since they often have to be made over a period of time to allow for the approach to thermal equilibrium, it may be more efficient to pull the rod and sampling equipment immediately and to measure temperature in a separate hole. A convenient and inexpensive way of making the hole is to use the drive rod to set a continuous length of polyethylene tubing. The tubing is threaded through successive lengths of drive rod when they are added. When the desired depth is reached, the rod is pulled, leaving behind the tubing and an expendable drive point to which it is attached. The temperature measurements are made inside this tubing with a thermistor in a small diameter housing. Additional details of the temperature-measuring methods and equipment are given by Osterkamp and Harrison [1981]. Water pressure measurements are made either by using the equipment as a standpipe piezometer or by using a commercial piezometer connected to the top of the probe.

The equipment is described briefly in the next section. More details are available in a report by Harrison et al. [1980], and detailed drawings will be supplied upon request. That report also outlines a method for estimating when contamination by drilling water is likely to be a problem in a more standard soil and water sampling procedure.

DESCRIPTION

Drive Rod and Tubing

The sampler is attached to the bottom of a string of 5-ft (1.52-m) sections of standard EW or A drill rod. Because the drill rod may leak between sections, polyethylene tubing is used inside it to connect the sampler to the surface. A section of tubing is added with each section of drill rod using standard fittings (Swagelok, Crawford Fitting Co., Solon, Ohio). The end of the top section of tubing passes out